Annals of Biomedical Engineering, Vol. 40, No. 2, February 2012 *(© 2012)* pp. 346–366
DOI: 10.1007/s10439-011-0501-4

BMES BIOMEDICAL ENGINEERING SOCIETY™ www.bmes.org

Optical and Opto-Acoustic Interventional Imaging

ATHANASIOS SARANTOPOULOS, NICOLAS BEZIERE, and VASILIS NTZIACHRISTOS

Institute for Biological and Medical Imaging, Technische Universität München & Helmholtz Zentrum München, Munich, Germany

(Received 28 September 2011; accepted 23 December 2011; published online 7 January 2012)

Associate Editor Daniel Elson oversaw the review of this article.

Abstract—Many clinical interventional procedures, such as surgery or endoscopy, are today still guided by human vision and perception. Human vision however is not sensitive or accurate in detecting a large range of disease biomarkers, for example cellular or molecular processes characteristic of disease. For this reason advanced optical and opto-acoustic (photo-acoustic) methods are considered for enabling a more versatile, sensitive and accurate detection of disease biomarkers and complement human vision in clinical decision making during interventions. Herein, we outline developments in emerging fluorescence and opto-acoustic sensing and imaging techniques that can lead to practical implementations toward improving interventional vision.

Keywords—Surgery, Endoscopy, Intra-operative imaging, Surgical imaging, Optical imaging, Fluorescence, Opto-acoustic, Photoacoustic.

INTRODUCTION

Bio-engineering, bio-technology and associated technologies have seen a continuous growth over the past decades by the development of concepts and tools that advance our understanding of life and disease. From system biology approaches to advanced diagnostic and therapeutic strategies, there is an increasing sophistication in approaches geared toward finding effective treatments and curing major diseases. It comes then often as a surprise when one realizes that for a large part of medical visualization, for example in surgery, endoscopy and overall in interventional procedures, the most widely used detector is the human eye; a process that has remained unchanged for thousands of years.

Address correspondence to Vasilis Ntziachristos, Institute for Biological and Medical Imaging, Technische Universität München & Helmholtz Zentrum München, Munich, Germany. Electronic mail: v.ntziachristos@tum.de

The human eye is an excellent detector of anatomical features and it can also detect certain major discolorations. Overall however, human vision is not appropriate for visualizing many molecular diseases. Limitations are typically related with inabilities in visualizing molecules and genes, small clusters of cells and cellular function or seeing under the surface. Radiological approaches have been considered for improving on the visual examination during interventions. Magnetic resonance imaging (MRI),[11,40,45,137,142,201] positron emission tomography (PET),[5,13,32,80,115,133] ultrasound (US)[61,151,155,163] and X-ray computed tomography (CT)[20,26,65,149] offer several promising characteristics but also come with limitations. Most whole-body imaging methods are of substantial size and cost that limits them from gaining wide dissemination in the operating room and they do not typically offer imaging resolution that matches that of the human eye (i.e., ~50 μm, or better when using surgical microscopes). US imaging and portable gamma cameras are potent methods for imaging during interventional procedures as they offer practical implementations; in particular they are portable and can be built in small form factors and in a cost-efficient manner. Despite their advantages over larger radiological systems, clinical decision making during surgery or endoscopic intervention still relies primarily on the surgeon's ability to distinguish cancerous from healthy tissue under visual examination, palpation and corresponding histopathological confirmation.

Advanced optical imaging approaches have been considered as alternatives that can enhance interventional imaging as they directly relate to surgical vision and can offer resolutions that match or exceed that of the human eye. Of particular importance is the ability to generate contrast from disease that goes beyond sensing discolorations or the anatomical features that can be perceived by the human eye so that additional diagnostic or theranostic information is provided during the imaging session. Improved contrast can be

achieved by using exogenous contrast agents tailored to highlight certain biological events or functions, or by detecting disease-related endogenous optical contrast that goes beyond the discrimination sensitivity of human vision. The ability to integrate optical methods in existing endoscopes could further allow a seamless operation in the operating suite.

This review discusses optical imaging approaches developed to enhance interventional imaging. While particular concentration is given to cancer imaging approaches, the methodologies developed apply more generally to detecting a larger range of diseases spanning from cardiovascular disease to infection or nerve imaging. This is because the improvement of optical identification of cancer during surgery closely relates to the ability for early diagnosis during screening endoscopy or for identifying inflammation or infection during interventional procedures in cardiovascular applications, anastomosis procedures and so on. The optical imaging approaches considered for interventional imaging are divided herein based on their operational characteristics into two main categories, i.e., optical imaging implementations that offer large field of view inspection (several cm × cm) and methods that operate with smaller field of view but offer higher resolution and three-dimensional tissue visualization through several hundreds of microns to centimeters.

Large Field of View Optical Methods

Narrow Band Imaging

Narrow band imaging (NBI) is a method primarily used in endoscopic systems of the digestive tract to increase/enhance local changes in tissue absorption using spectral differentiation in epi-illumination (reflectance) geometry. Typically systems capture images at spectral bands around 415, 540 nm and possibly 600 nm and offer processed images that are a fusion of the spectral images captured. The principle of operation relies on the differences in light penetration for blue light (415 nm) vs. green light (540 nm). In response, narrow band blue light images are sensitive to superficial blood vessels, while green light images contain contrast from deeper (sub-epithelial) blood vessels. NBI can therefore highlight superficial microvasculature differences and the underlying mucosal tissue of superficial suspicious lesions up to 200 μm depth. The irregular shape, size and pattern of local microvasculature (vessels and capillaries) and disrupted tissue structure associated with pre-cancer or early cancer development can thus be visualized with increased sensitivity and contrast from the surrounding tissues, compared to white light endoscopy (WLE). Studies report that NBI has been found superior for the detection of colorectal,[46,86,87,208] gastric,[23,98] lung[221] cancers or precancers and Barrett's esophagus[214] with enhanced sensitivity and specificity compared to WLE. Figure 1 illustrates the contrast increase when using NBI compared to WLE in an intestinal metaplasia case. Kato *et al.*[98] demonstrated the performance of NBI in 201 lesions from 111 patients with a high risk of gastric cancer. Using a magnifying endoscopy NBI system, they achieved a sensitivity and specificity of 92.9 and 94.7%, respectively in identifying gastric cancer, compared with 42.9 and 61.0% of WLE.

Despite the simplicity of implementation and use, NBI is still under evaluation as many studies suggest that although NBI offers an alternative, 'contrast-enhanced' visualization of the tissues, this technology has limited specificity,[23,96] moderate inter-observer agreement,[36,86] requires considerable learning experience[46] or does not present a comparable advantage compared to the latest high resolution white light endoscopy (HR-WLE)[35,157] or even conventional colonoscopy[2] systems. To overcome these limitations some approaches adopted a multimodal

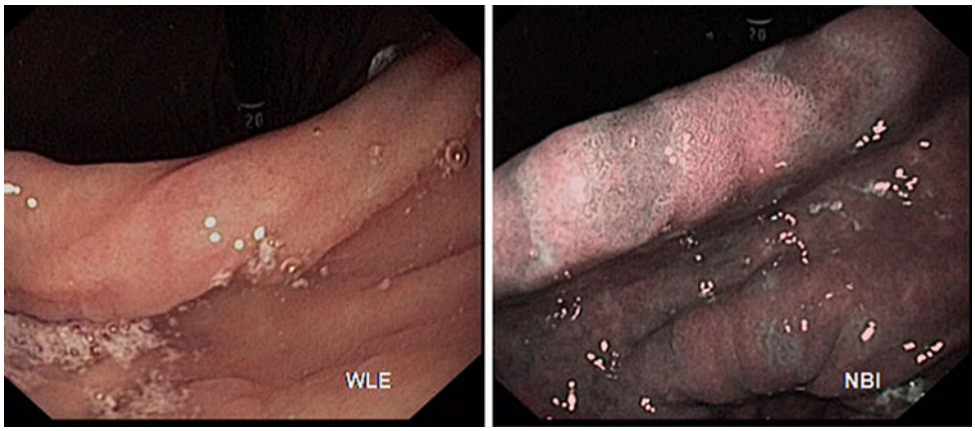

FIGURE 1. White light endoscopy (left) observation of intestinal metaplasia at the angulus, and contrast improvement from NBI (right) of the same region.

solution by combining NBI with other techniques (auto-fluorescence, chromoendoscopy or HR-WLE)[37] to improve the overall system performance.

Auto-Fluorescence Imaging (Endogenous Contrast)

Auto-fluorescence, i.e., the fluorescence emitted by endogenous tissue molecules, may vary between different tissues, for example during tissue progression from healthy to malignant. Collagen, nicotinamide adenine dinucleotide (NADH) and flavin adenine dinucleotide (FAD) are predominant intrinsic tissue molecules that emit fluorescence upon excitation with UV or blue light.[42,63] Alterations in the biochemical composition of tissue during the early stages of carcinogenesis can be observed as a change in the fluorescence signals captured indicating cancer-associated tissue changes. Various wavelengths for both the excitation (300–480 nm) and emission (500–700 nm) of intrinsic fluorophores have been utilized (especially for auto-fluorescence spectroscopy), but typically blue light excitation (~450 nm) is preferred to UV light, due to the low UV transmittance of conventional optics. The fluorescence emission captured then at lower energies, typically in the green but also in the red spectral regions. Tumor appearance is manifested as a reduction of the green fluorescence (due to collagen cross-links breakdown) and an increase in the red fluorescence (due to an increase of local porphyrins).[100,116,121] Auto-fluorescence imaging is technically easy to implement during patient screening or surgery and therefore it does not require expensive equipment or complex regulatory approvals. Endoscopic and wide-field auto-fluorescence imaging has been considered for screening oral,[38,83,90,117,161,175] laryngeal,[8,112,220] cervical,[54,84,193] gastric[55,72] and colorectal[88,186] cancer. Lane *et al.*[117] reported a 98 and 100% increase of sensitivity and specificity using autofluorescence imaging in 44 patients screened for oral dysplasia or cancer, while Kraft *et al.*[112] observed a superior performance of autofluorescence (sensitivity 91%, specificity 84%) endoscopy compared to white light (sensitivity 73%, specificity 79%) and even aminolevulinic acid (ALA) induced fluorescence (sensitivity 95%, specificity 62%) endoscopy. Auto-fluorescence images of a papillary tumor showcasing the contrast improvement achieved are shown in Fig. 2.

Currently, however, opinions are divided as to the specificity of the technique. Huh *et al.*[84] reported a specificity of 50% in a 604-patient study for cervical neoplasia, while Jayaprakash *et al.*[90] presented similar specificity in 60 high risk patients with suspicious oral lesions. It is hypothesized that biological mechanisms other than tumor-related biochemical changes can also cause a reduction in green fluorescence, presenting, thus, false positives. Inflammation, pigmentation, hyperkeratosis and ulceration are all conditions under which a decrease in green fluorescence levels can be observed, rendering thus the identification of malignant lesions challenging. In addition, as discussed in the following, fluorescence imaging depends on many instrumentation and tissue parameters and data currently are not performed using standardized performance; a topic that is not accurately considered yet in clinical studies but can lead to data variability.

Hybrid approaches have been also considered for bypassing these limitations, for example the combination of autofluorescence imaging and NBI have been proposed[97,161] for utilizing narrow band images to reduce the false positive rate of the autofluorescence modality (from 40% to only 10%).

Epi-Illumination Fluorescence Imaging (Exogenous Contrast)

In addition to utilizing endogenous tissue contrast, the field of targeted fluorescent agents for exogenous

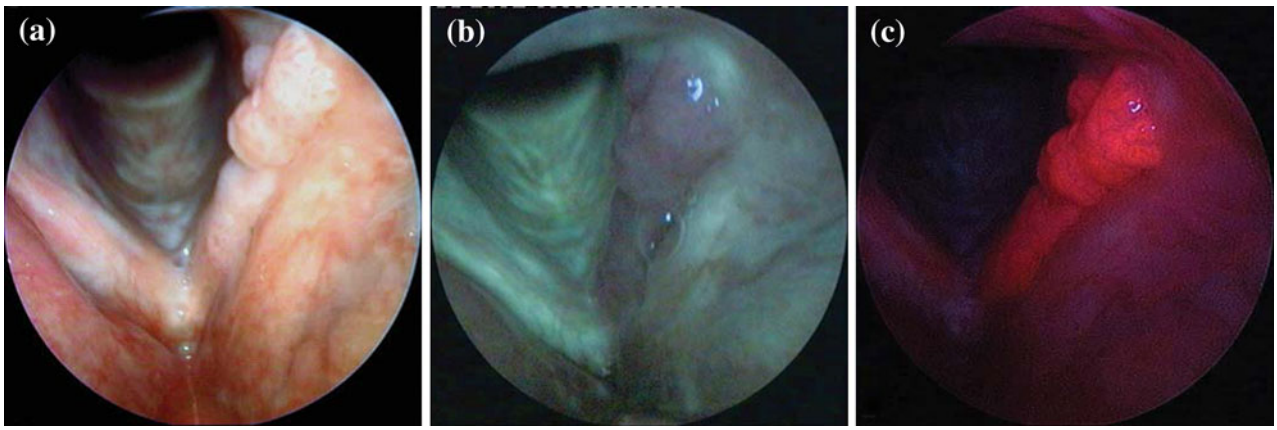

FIGURE 2. Respiratory papilloma images obtained from WLE (a), demonstrating a papillary tumor of the left vocal fold; Autofluorescence Endoscopy (b), showing a marked loss of autofluorescence; Induced Fluorescence Endoscopy (c), displaying a strong protoporphyrin IX fluorescence.

administration has exploded in the last decade. The administration of fluorescent contrast agents, i.e., nonspecific dyes that distribute primarily in the vascular system, has been considered since the 1940s using fluorescein.[114] Fluorescein is a nonspecific organic fluorophore with an absorption maximum at 494 nm emission maximum at ~521 nm. Due to the high absorption of visible light by hemoglobin, fluorescein can be detected generally in superficial tissues (< 5 mm). Fluorescein is primarily used in eye diagnostics and retinal angiography studies,[25,57,191] including measurements of retinal perfusion[177] but its use in other applications has been considered for example in cranial base surgery,[152] thoracoscopy,[143] glioma surgery,[114] colorectal cancer[124] or to monitor aortic valve replacement surgery.[159]

In addition to fluorescein, indocyanine green (ICG)[168] has also been considered as an alternative organic dye for optical imaging applications operating in the near-infrared. Since operation in the near-infrared allows imaging deeper than in the visible, ICG has been more recently employed in several interventional applications, for example for sentinel lymph node (SLN) identification in breast,[202] gastric,[101] cervical[34] and vulvar[33] cancer, for angiography during reconstructive surgery,[39,73,113,185,210] skin flap perfusion,[78] lymphatic drainage mapping[1,172] and for imaging of glioma[70] and liver cancer[66,89] and metastases.[203] Results obtained with ICG during a hepatectomy procedure can be seen in Fig. 3.

Both fluorescein and ICG are organic dyes with the ability to visualize the vascular system. Their consideration for cancer imaging relates to possible retention of the dye by tumors, due to the enhanced permeability and retention (EPR) effect of tumor vasculature.[66,89,147] In particular for ICG, Ishizawa *et al.*[89] noted that after i.v. injection ICG was retained in hepatocellular carcinoma (HCC) as a result of biliary excretion disorders in cancerous tissues. The subsequent study included 49 patients and confirmed that tumor imaging of HCC and of metastases of colorectal carcinoma is feasible with this—otherwise tumor unspecific-technique. In another study, Adams *et al.*[1] successfully tracked the lymphatic propulsion of an ICG micro-dose in patients suffering lymphedema and could evaluate treatment efficacy.

Despite the relatively wide use of organic dyes for *in vivo* staining of tissue vasculature, their use in detecting major diseases has not yet shown of high clinical relevance. To differentiate genetic diseases based on more specific biochemical signals, photosensitizers have been considered for intra-operative detection. In particular, administration of 5-aminolevulinic acid (ALA) induces

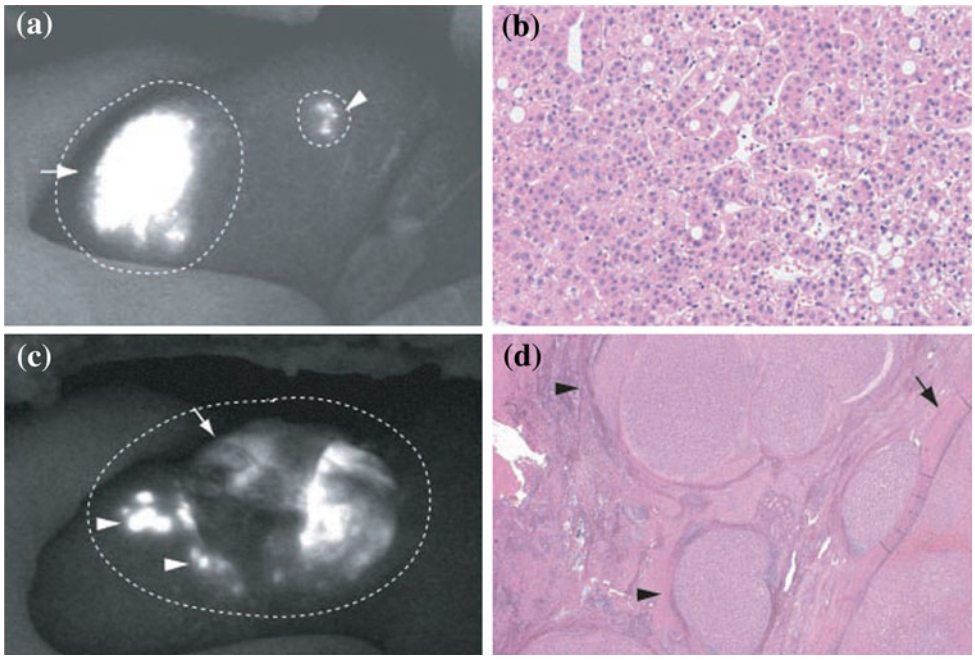

FIGURE 3. Hepatocellular carcinoma cases observed using fluorescence imaging and confirmed by H&E staining. (a, b) Hepatectomy procedure in a 59 years old patient suffering from HCC. a Intraoperative ICG fluorescence imaging technique shows bright signals in the primary HCC nodule (thin arrow) and a new single nodule (arrowhead). White broken lines show the planned liver resection line. (b) A photomicrograph of the new single nodule section stained by H&E (original magnification, ×100). (c, d) Hepatectomy of a case of HCC in a 75 years-old patient. (c) Intraoperative ICG fluorescence imaging technique shows bright signals in the primary HCC nodule (thin arrow) and new multiple nodules (arrowheads). A white broken line shows the planned resection line of liver. (d) A photomicrograph of the new multiple nodules (arrowheads) section stained by H&E (original magnification, ×10).

tissue fluorescence by enabling the production of porphyrins in cancer cells, a process that has been studied for intra-operative identification of gliomas of grade III or IV.[52,85,136,181,199,211] Stummer *et al.*[181] in a randomized multicenter clinical trial included 322 patients and reported a 65% complete tumor resection for the ALA administered patients compared with only 36% tumor removal under white light guidance. In addition to glioma surgery, ALA-induced protoporphyrin IX (PpIX) has been also shown potent in the detection of bladder cancer[85,93] and of basal cell carcinoma.[59,166,215] Remarkably, the hexyl-ester of ALA, hexaminolevulinate, has shown an interesting impact on fluorescence cystoscopy in patients presenting non-muscle invasive bladder cancer, increasing the detection and surgical outcome of bladder cancer resections.[130,212,213]

On top of the detection improvement induced by the use of such compounds, they enable *in situ* photodynamic therapy. Such a strategy of using intense light to destroy cancerous cells with photosensitizers is currently used in several cancers (head, neck, esophagus, skin, lung, biliary tract) [43,53,64,91,222] with a variety of photosensitizers, mostly porphyrin derivatives, such as Photofrin[134] of Foscan,[160] and porphyrin precursors such as the previously cited ALA.[127]

Finally, an important class of exogenous fluorescent agents relates to targeted agents with specificity to cellular and molecular targets. A common form of such agents relates to labeled antibodies and anti-body fragments but significantly more elaborate chemistries have been considered, including activatable probes, i.e., probes that are dark in their base state but fluorescence after interaction with a molecular target. These probes can reveal specific characteristics of complex disease such as cancer, atherosclerosis and other multi-factorial diseases, by illuminating changes in the expression profiles, signaling pathways and other molecular abnormalities. A significant advantage of this approach is that contrast can be engineered so as to reveal specific tissue and disease bio-markers. In that respect it can capitalize on "-omics" approaches and large scale discovery of disease profiles at the systems level. Despite however of the strong potential of the approach, an important limitation concerns the navigation of the corresponding regulatory procedures and ultimately the safety of these agents for human use. The particular issue in this case is the risk associated with the clinical translation of such agents to human. Conversely with the first clinical translation of a folate targeting agent has been now achieved[204] and demonstrated on surgery of ovarian cancer patients, a significant milestone associated with the clinical translation of targeted agents has been reached, hopefully serving as a stepping stone to the translation of additional agents enabling a larger disease targeting ability.

Quantitative Fluorescence Imaging and Data Standardization

Fluorescence imaging systems typically comprise of an illumination source emitting continuous wave (CW) light at one or multiple wavelengths (or spectral bands) and a lens-based charge-couple device (CCD) camera using appropriate filters for imaging the fluorescence emitted from tissue.[18,146,194] The most common operation mode is epi-illumination, whereby the source and the detector are on the same side of the object imaged. Several variations of this approach have been considered, a common approach being the combination of a fluorescence sensing camera and a color camera.[194]

Although planar fluorescence imaging appears straightforward to implement and interpret, preclinical and clinical studies have demonstrated several limitations, which compromise accurate fluorescence quantification in common epi-illumination implementations.[18,146,179] Perhaps the most important aspect is that the fluorescence images captured do not reflect the true fluorochrome bio-distribution, but rather a mixed contribution of fluorochrome bio-distribution and tissue optical properties, i.e., absorption and scattering. In this way, variations of tissue optical properties for example will modify the fluorescence image and may lead to artifacts and interpretation errors. Tissue absorption variations typically relate to oxygenated and deoxygenated hemoglobin (HbO_2 and Hb) concentration differences between tissues or lesions whereas tissue scattering variations relate to cellular density and morphology diversity among them. For example a typical problem during surgery is the presence of blood on the lesion that attenuates the fluorescence signal, but such effects can more generally occur when imaging lesions of different vasculature and cellular density are imaged, which implies different amounts of hemoglobin and scattering within the lesion.

Overall methods that overcome these limitations, for example ratiometric fluorescence imaging approaches[15,194] are important to offer accurate performance and enable data standardization, an important aspect for multi-center clinical trials. These approaches are implemented as multi-spectral methods, simultaneously collecting in different spectral bands and processing the data, preferably in real-time, in order to provide accurate fluorescence images. A three-imaging-channels approach, where color, fluorescence and attenuation measurements are simultaneously captured and processed was introduced for correcting for absorption variations of tissue in the surgical field.[194] In this case the light-absorption correction is based on a ratio of fluorescence over light attenuation images and the system performance was illustrated in *in vivo* studies. Figure 4 illustrate this three channels method using an exogenous contrast agent to highlight

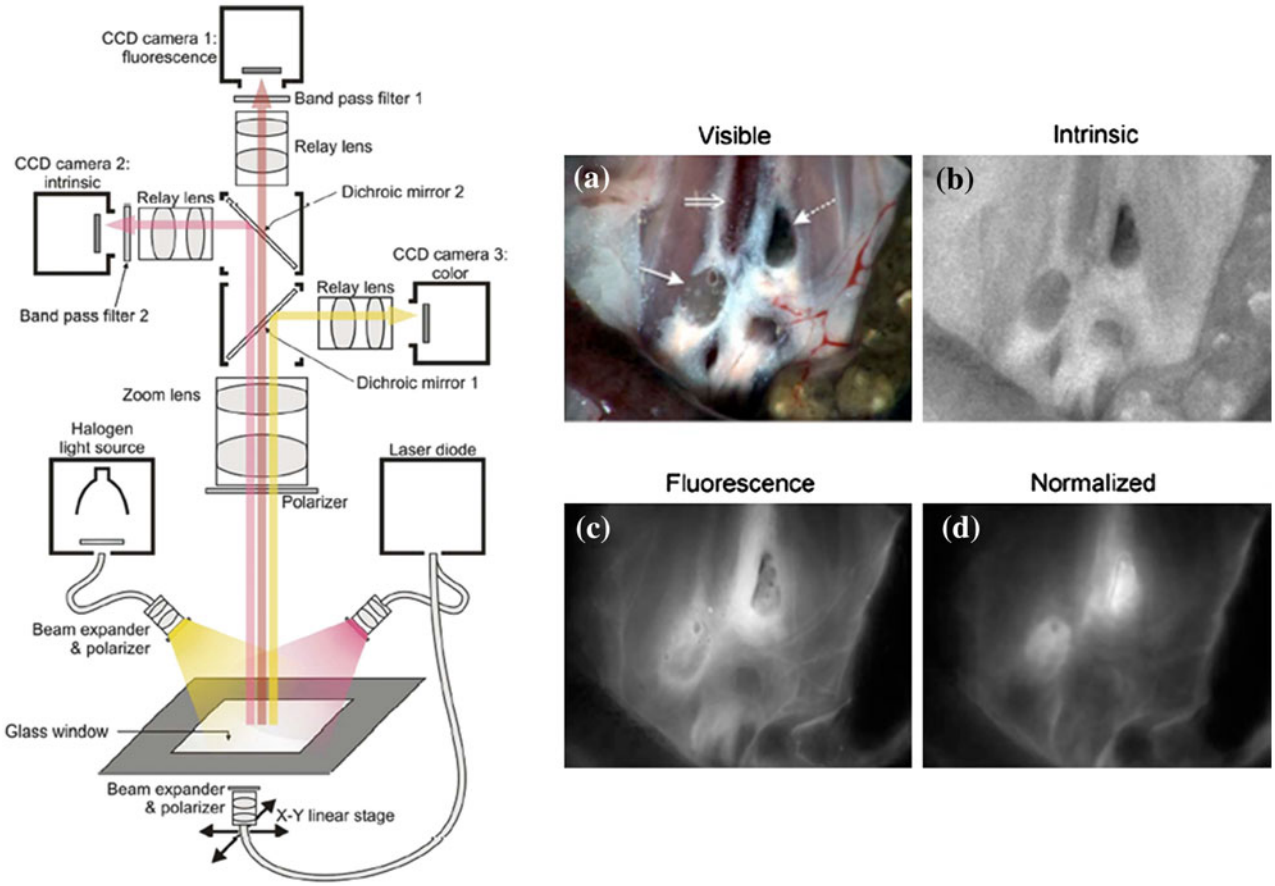

FIGURE 4. Quantitative fluorescence modality. As shown on the left hand side, the apparatus encompasses three cameras to acquire, respectively color, intrinsic fluorescence and excitation fluorescence epi-illumination images using adequate filters for the beam and provide through data processing normalized fluorescence images (where the instrinsic signal is removed from the fluorescence signal) in real time.[194] Postmortem imaging of the surgically exposed mouse abdominal area in epi-illumination mode allows the simultaneous acquisition of: (a) a color image showing the lumbar lymph nodes around the inferior vena cava; (b) an image obtained at the excitation wavelength (intrinsic image), showing absorption differences between the two lymph nodes due to the differential injection of an absorber; (c) a conventional fluorescence image showing low signal intensity from the lymph nodes compared to bright background signals; (d) normalized image displaying markedly improved fluorescence quantification, correctly resolving the underlying fluorescence activity in the nodes.

the lymph nodes in a mouse model. Other methods have considered a double ratiometric technique, where attenuation and fluorescence images were captured for two different excitation wavelengths and were subsequently utilized in phantoms and clinically in patients undergoing prostatectomy.[16] The ongoing work pioneered by Andersson-Engels and co-workers in the field of fluorescence data processing is currently in the process of clinical translation for real time monitoring of cancer treatment.[94,184]

It is also possible to highlight the localization of fluorescent probes using fluorescence lifetime-resolved imaging.[29] Recent advances have even pushed this method to *in vivo* samples, with an emphasis on intraoperative methods, albeit with a restricted field of view.[74,176,182] It capitalizes on the different of lifetime of the fluorescent probe with the background fluorescence, as well as the difference of lifetime of the contrast agent depending on its immediate surroundings which is interesting in the case of fluorescent metabolites and activatable probes.[197] Time-gated spectroscopy, aiming at separating photon based on their scattering pathway, is also being investigated by different groups *in vivo* and presents interesting results.[12,183,200]

Overall, the development of methods that account for photon tissue interactions in real-time are increasingly considered, especially in association with a broader acceptance of fluorescence imaging in intraoperative procedures.

Opto-acoustic Imaging

Opto-acoustic imaging is a hybrid imaging modality, using light as a source and acoustics for signal detection. Its major advantage is that image formation is not limited by photon scattering, since no photons but US waves are detected. Therefore the resolution of

this optical imaging approach is defined by the US diffraction limit and can reach a few tens of microns or better. When a molecule is illuminated with light pulses (typically in the nanosecond range), the transient temperature increase causes a thermoelastic expansion. This in turns generates ultrasonic waves, ranging from a few kHz to several MHz, which can be detected by ultrasonic detectors After data treatment by mathematical procedures, an image of optical absorption inside tissue can be obtained.[144] If a single wavelength is used, mapping of strong endogenous absorbers is possible, such as blood or melanin. The detection of exogenously administered chromophores is also possible especially with multi-spectral illumination techniques. Multispectral opto-acoustic tomography (MSOT) collects data after illuminating tissue at multiple wavelengths, and by applying spectral processing techniques it can then derive images of the distribution of different optical dyes or targeted probes *in vivo* through tissues at US resolution.[145] It has been shown that detection of optical contrast can be imaged with resolutions of 30–40 μm through at least 4–6 mm of tissue.[81] Deeper penetration through 1.5–2 cm has been also achieved with resolutions at the 100–200 μm range. Video rate imaging has also shown possible and has been demonstrated in visualizing kidney perfusion in mice,[21] as shown in Fig. 5 or in studying tumor vascularization.[95] High-resolution video rate optical imaging through several millimeters to centimeters of tissue penetration are the characteristics of a method with great potential toward interventional imaging.[41] Several clinical implementations can be foreseen following the general hardware characteristics of corresponding ultrasonic probes with the addition of light generation and guiding components to impart opto-acoustic responses. Handheld devices for opto-acoustic imaging have been described so far, also in setups that also implement conventional US imaging.[141] Endoscopic imaging for the upper and lower gastro-intestinal tract, vascular imaging and in general hollow organ imaging have also been proposed.[217] Overall, the imaging and clinical outcome performance of these approaches needs to be established.

Opto-acoustic interventional imaging can prove useful in a number of applications, such as micro-vasculature characterization,[82] blood oxygen saturation and volume mapping and imaging of the bio-distribution of optical agents employed to outline anatomical, functional or molecular disease biomarkers. A wide array of optical agents can be employed spanning from carbon or gold nano-particles to organic dyes or even fluorochromes.[104] These reporter molecules can be considered as stand-alone or as labels of molecules, antibodies or antibody fragments in order

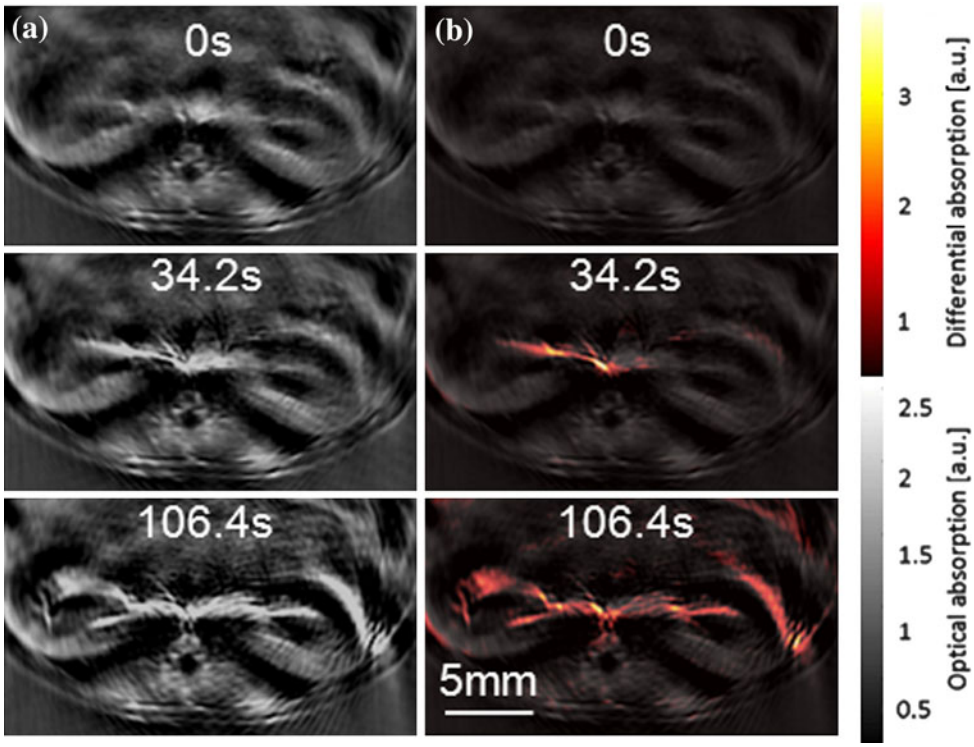

FIGURE 5. Perfusion of a mouse kidney with indocyanide green imaged by opto-acoustic tomography. On the left panel (a), images obtained by opto-acoustic tomography at 800 nm illumination wavelength. On the right panel (b), image difference at different wavelength to highlight ICG distribution overlayed on the image acquired a 800 nm.

to target specific cellular and sub-cellular characteristics of a disease. For example organic dyes can be used to outline reconnected vessels and visualize flow and perfusion. Functionalized dyes or nano-particles can also label moieties that bind specific cellular receptors, in order to target a set of biomarkers. Nanoparticles, such as gold nanorods[198] and carbon nanotubes,[132] are known to be good light absorbers in the near infra-red region of the light spectrum. They can, similarly to purely organic contrast agent, be chemically modified to display specific properties such as a targeting capacity. On top of that, they can also be used as nanocarriers for drugs,[164] or as photodynamic therapy agents in cancer treatment.[27]

Opto-acoustic imaging is a highly scalable approach since depth can be exchanged for resolution: the more superficial the imaging the higher the resolution achieved and *vice versa*. Microscopic implementations using opto-acoustic have been described since the early 70s. However microscopic implementation also come with reduced fields of view; therefore in principle opto-acoustic imaging can also be considered in the context of the microscopic methods that follow in the next section.

Microscopic Optical Methods

Optical Coherence Tomography (OCT)

Optical coherence tomography, developed during the last two decades, is an optical approach that maps local changes in the refractive index of a tissue in 2D and 3D. It is usually exemplified as the optical version of US, whereby it detects depth-resolved local reflectivity of biological samples by utilizing interferometry. OCT provides real-time imaging of tissue structures (morphology) with high resolution (1–15 μm), while its penetration depth, limited by the scattering properties of the tissue and the wavelength used, in biological samples is typically around 1–2 mm. Many novel implementations of OCT systems are developed in order to incorporate functional properties to the technique. Thus, novel OCT systems are able to distinguish between polarization (PS-OCT)[106] and phase differences[190] or feature Doppler capabilities[178,218] for blood flow imaging allowing, thus, the detection of more disease-related tissue properties. OCT has found diverse applications in clinical research and is widely used predominantly in ophthalmology for the screening of various diseases,[10,105,188,219] providing an useful non-contact diagnosis tool, but also in dermatology[67,77] and cardiology[6,126,156,189,216] where clinical translation is ongoing.[79] Figure 6 shows images of the human retinal micro-capillary network obtained by classical fluorescein angiography and phase-variance OCT for comparison purpose.

Optical coherence tomography endoscopes have emerged, based on optical fibers for light delivery and detection. OCT endoscopes have been described in combination with imaging of the gastro-intestinal tract[51,106,218,227] or the larynx[22,173] for tumor detection as well as in cardiac intra-vascular imaging for imaging atherosclerotic plaques or stents,[19,227] the latter being particularly useful for post-implantation monitoring of stent status. OCT has also been considered in the context of surgical procedures with applications to lymph node and tumor imaging.[138] Gallwas *et al.*[58] investigated the capability of OCT to detect and differentiate between various stages of cervical intraepithelial neoplasia (CIN) using colposcopy for the OCT guidance. OCT imaging results for 120 patients compared with histology, showed 86% sensitivity and 64% specificity using CIN grade 2 as a threshold. A larger

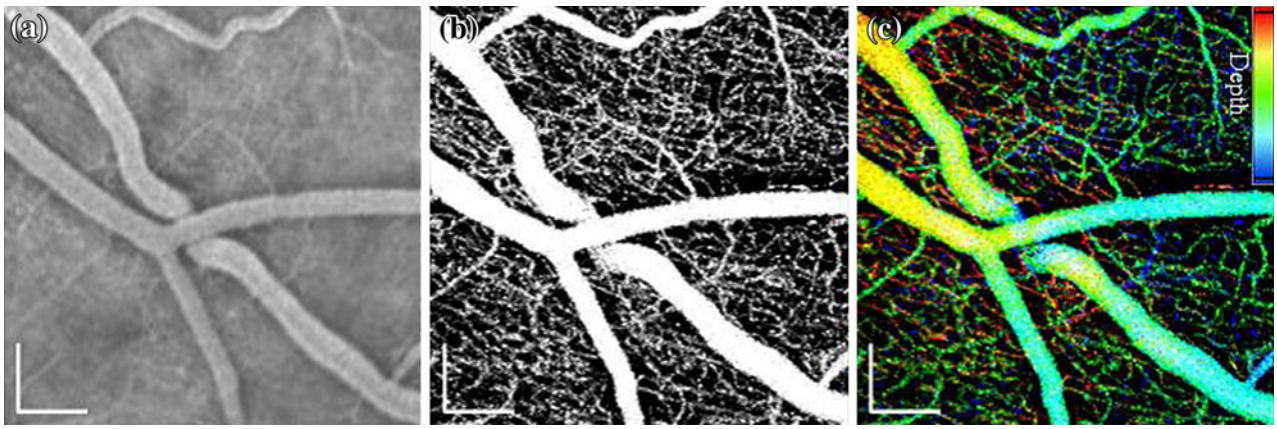

FIGURE 6. ***In vivo*** **human retinal micro-capillary network images. Image size is 1.5 × 1.5 mm^2. (a) Fluorescein angiography. (b) Projection view of retinal contributions to phase-variance (pvOCT). (c) RGB depth color-coded projection view of retinal pvOCT data. Upper right shows depth scale bar with red color denoting a top layer, green showing capillaries as an intermediate vascular bed, and finally blue represents micro-capillaries as a deeper vascular plexus layer. The imaging acquisition time of pvOCT is 3.5 s. Scale bar: 250 μm.**

number of applications have been reviewed by Marschall *et al.*[131] Multi-modal implementations using OCT have also been suggested for improving imaging performance, for example the combination of OCT with multi-photon tomography,[109,207] Raman spectroscopy, or opto-acoustic imaging.[123]

In the recent years, *in vivo* optical coherence microscopy (OCM) started appearing[3,28,120] and making their way into hand-held probes,[4,110] to try to overcome to transverse resolution limit of classical OCT, albeit with a more limited field of view. In that respect, it becomes complementary to confocal microscopy (CM) since it relies on different contrast sources and presents different imaging properties depending on sample thickness.

Endoscopic Confocal Microscopy

Confocal microscopy provides optical diffraction-limited resolution imaging even when imaging thick tissues; it is therefore appropriate for *in vivo* imaging applications, in contrast to conventional microscopy which requires tissue slices of 5–10 μm in order to offer high resolution imaging. CM rejects scattered photons by means of a small pinhole aperture placed in front of the detector. The implementation of CM around flexible fiber-based endoscopes has enabled the clinical propagation of the technology, since the flexible endoscope can be brought in contact with tissue to investigate the area under it. Although limited field of view can be achieved (<mm), endogenous and exogenous contrast agents can be visualized in high resolution (<1 μm lateral; <10 μm axial), within the first 100 μm of tissue. Typical frame rates achieved is in the few Hz. CM makes use of autofluorescence,[102,195] or extrinsically administered agents including fluorescein,[75,103,206] ALA-induced PpIX,[196,224] the fluorescent agent acriflavine[187] for confocal fluorescence imaging, or acetic acid[24,30,129,187] has been locally applied to cause "brightening" of the cell nuclei which, in turn, enables the visualization of changes in nuclear size and density, and N/C ratio (nuclei to cytoplasm).[128] Typical images obtained by this method are presented and compared to classical H&E staining in Fig. 7. Collier *et al.*[30] reported 100% sensitivity and specificity for 28 fresh samples from patients with cervical intra epithelial neoplasia using acetic acid for the contrast build up and a processing algorithm for the scoring. Furthermore they introduced and evaluated various metrics for the classification of tissue samples based on nuclear size and cell separation distance.

Confocal imaging has been considered in many clinical applications, including the detection of oral,[24,75,129,196,224] cervical[30,187] or skin[62] cancer, Barrett's esophagus[103,154] and in ophthalmology.[48,102] Haxel *et al.*[75] used a flexible confocal endoscope to image the oral region after i.v. injection of fluorescein and could successfully discriminate cancerous and healthy tissue, while Kiesslich *et al.*[103] reported a sensitivity and specificity of over 95% in

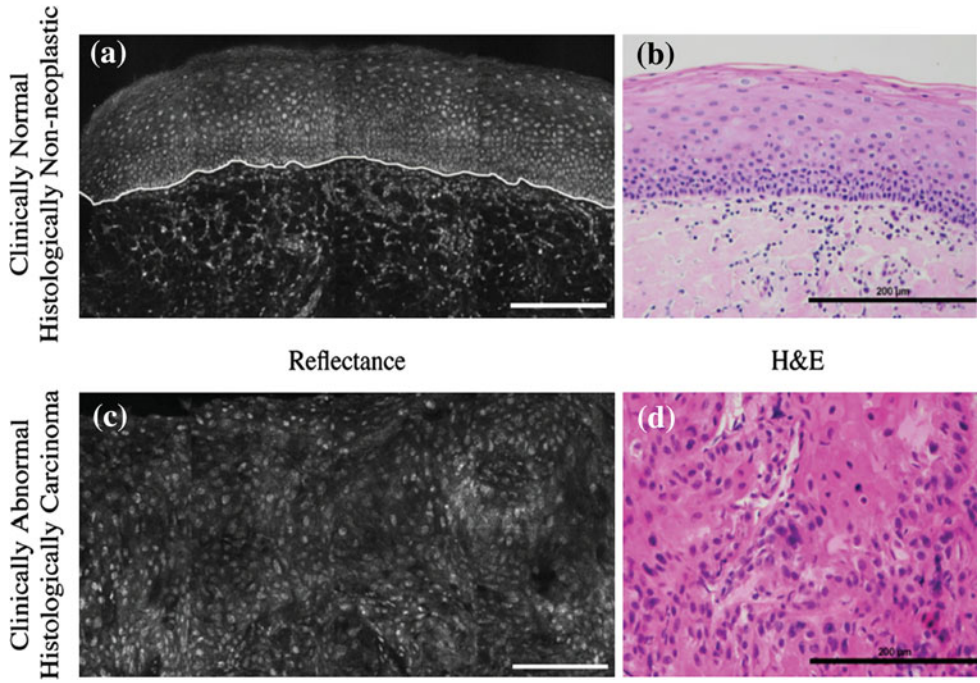

FIGURE 7. (a, c) Confocal reflectance and (b, d) H&E images of tissue slices from oral mucosa biopsies of the same patient. Confocal images were taken after applying 6% acetic acid to the tissue slices. The white line in image (a) defines the basement membrane. White circular structures in the confocal images are cell nuclei. Scale bar: 200 μm.

63 patients screened with confocal fluorescence microscopy for Barrett's esophagus. Finally, others followed dual-contrast approaches for real-time histology, by simultaneously using fluorescein and acriflavine[206] or acriflavine and *ex vivo* specific molecular agents[24] and compared them to histological staining.

Confocal microscopy is limited to imaging only a few tens to a few hundred of microns deep. This reduces the applicability of the method in imaging large volumes. CM can nevertheless provide a useful tool for high-resolution local imaging of suspicious areas and has been proposed for defining resection perimeters in oncology in real time,[139] also in combination with the use of exogenous contrast agents, for example in neurological oncology.[165] The clinical interventional application of the method may be significantly augmented when applied in combination with large field of view methods, in particular fluorescence imaging, the latter used to guide CM imaging to suspicious tissue segments.

Nonlinear Microscopy (2-Photon Microscopy, Second Harmonic Generation, CARS)

Nonlinear microscopy offers several attractive imaging characteristics and is considered as an alternative to confocal imaging. 2-photon microscopy (2PM) and second harmonic generation (SHG) are nonlinear phenomena of photon-tissue interaction. 2PM refers to the simultaneous absorption of two photons of long wavelengths that causes a fluorescence emission of one photon of shorter wavelength. SHG describes the characteristic ability of some molecules to absorb two photons and subsequently scatter a photon of exactly double frequency (SHG) without energy loss.[76] Higher order interactions are also possible, such as in multi-photon absorption techniques. Although the nonlinear excitation process has been documented since the 1930 s, the first practical implementations developed with the advent of femtosecond (fs) lasers and became popular over the last two decades. As nonlinear phenomena are inherently rarer compared with linear phenomena (i.e., fluorescence), nonlinear imaging necessitates a photon flux concentrated in space and time. The major advantage of 2PM is that the typical excitation range for intrinsic fluorophores (and extrinsic that fluoresce in the green (i.e., GFP) wavelengths) is between 700 and 900 nm, allowing, thus, a deeper penetration inside the tissue (~1 mm) due to reduced absorption and scattering.[44,192] Although safety concerns need to be considered, in relation to the use of highly concentrated laser powers for signal generation, multi-photon microscopy is broadly applied to imaging cell cultures,[158] animals[68,99,169] or *ex vivo* human samples, in particular the skin.[7,69,92,103,108,162,205] It will however hinder its clinical *in situ* use. Ericson *et al.* also investigated drug delivery in the skin using 2PM.[47] Jiang *et al.*[92] investigated *ex vivo* healthy human samples from colon, stomach and skin tissue and imaged 2-photon excited autofluorescence and SHG-excited collagen using a 800 nm excitation. Additionally Rogart *et al.*[162] showcased the ability of multiphoton microscopy to image the autofluorescence of fresh, unstained colonic mucosa samples with higher resolution compared to CM. In the last couple of years, endoscopes for *in vivo* imaging based on the two-photon imaging technique have started to emerge, and have to ability to display sub-cellular details.[118] However, their use is currently limited to research, typically in ophthalmology.[223]

Coherent anti-Stokes Raman scattering (CARS) microscopy, the nonlinear analog of Raman spectroscopy, is a multiphoton tissue-photon interaction capable of imaging tissue-intrinsic molecular vibrations. Two picosecond lasers of different frequencies ('pump' and 'Stokes') interact with tissue to give rise to vibrations in resonant molecules resulting in a strong anti-Stokes signal. Being a nonlinear effect, the CARS signal is similarly confined in space and allows high-resolution three-dimensional imaging with sub-micron spatial resolution. It can be combined with other nonlinear techniques (2PM, SHG) and provide additional chemical information. So far, CARS has been used to image lipids and exogenous mineral oils[49,225] in cell cultures,[31,150,153,167,209] *ex vivo* and *in vivo* in small animals[49,50,56,119,125,153,225,226] or *ex vivo* human samples.[60] Recently Evans *et al.*[49] reported a CARS microscope capable of real time video rate imaging (20 fps) in small animals *in vivo*. They successfully visualized the lipid structure in mouse ear and recorded the perfusion of extrinsically administered mineral oil. Lim *et al.*[125] investigated the effects of high fat diet on atherosclerotic plaque formation in ApoE- deficient mice, using CARS, SHG and 2PM autofluorescence microscopies to image lipids, collagen and elastin, respectively. Figure 8 summarizes the theory behind non-linear optical microscopy and provides an example of a mouse aorta imaged by 2PM, SHG and CARS.

Ongoing research in the field of CARS microscopy aims to identify the suitable vibrational spectral regions that exhibit additional, medically relevant chemical and molecular signatures. Such generalization of the approach could open diagnostic and therapeutic applications, including applications to interventional imaging. Interestingly, CARS has been very recently combined with non-linear excitation of auto-fluorescence for application in dermatology.[107]

Point Spectroscopy (Reflectance, Fluorescence, Raman)

The term 'point spectroscopy' refers to fiber-optic implementations that measure spectra from confined

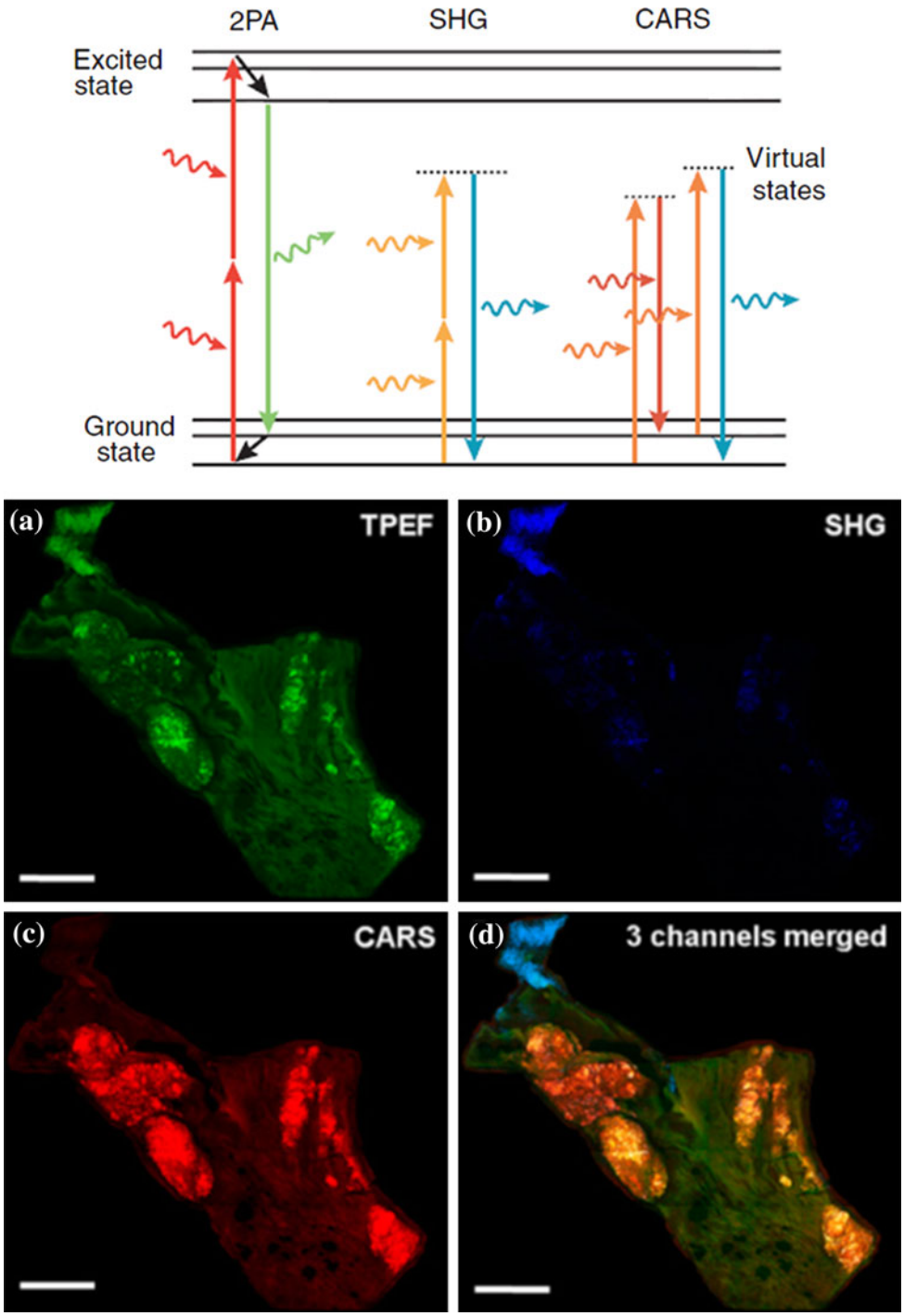

FIGURE 8. Two-photon absorption, SHG and CARS. Top: Jablonski diagram of the different modalities. Note that in second-harmonic generation and Raman scattering no actual electronic excitation takes place. Bottom: Representative composite images of the entire descending aorta in ApoE-deficient mice fed a Western diet. Images from three separate channels—Two-photon excitation fluorescence (a), SHG (b), and CARS (c)—were acquired simultaneously, with all three channels visible in (d). Each image consists of several individual image tiles, cropped and stitched together (approximately 8 × 10 tiles per composite image). Scale bar, lower left of each image = 500 μm.

"point" volumes on the surface of healthy and diseased tissues. Although not a purely 'imaging' technique, point spectroscopy provides detailed information regarding the back-reflected, fluorescence and vibrational (Raman) spectral properties of tissues. The acquired spectra are typically mathematically processed to reveal the exogenous[122] or endogenous tissue fluorescence, measure the local tissue absorption and scattering coefficients

(reflectance spectroscopy) or provide information about cell nuclei size (light scattering spectroscopy) and lipids (Raman). These tissue parameters represent biochemical and structural information and can offer information that can differentiate disease from healthy tissues. Point spectroscopy techniques have been used to detect breast,[71] oral,[122,135,170,171] brain,[17] cervical[63] and colon[174] cancer and atherosclerotic plaques.[167] Müller *et al.*[135] employed a tri-modal spectroscopy approach combining autofluorescence, diffuse reflectance and light scattering spectroscopy to distinguish normal from dysplastic and cancerous oral tissue. The study included 23 patients and showed that the method could differentiate between normal and malignant tissue with 96% sensitivity and 96% specificity and between cancerous and dysplastic tissue with 64% sensitivity and 90% specificity.

DISCUSSION AND CONCLUSION

The above presentation of bio-photonic technologies is not exhaustive of the existing literature on novel implementations, alternatives to these techniques and proof of principle studies. The methods presented however define major directions that have either considered in clinical studies or bring imaging performance that attains great promise for clinical application. Regardless, the clinical propagation and acceptance of optical technologies has been slow. One factor that affects this is that there is a large variety of photonic technologies, many of them developed with a technology-drive or a biological application drive but not around a clinical application. Therefore it becomes challenging to select the appropriate technology, match it with the complex and diverse requirements of a clinical need, and prove clinical impact. An additional limiting factor of clinical propagation is naturally the performance and accuracy of the method in resolving disease specific biomarkers.

Many researchers are increasingly orientating towards multimodal approaches in a 'best of both worlds' attempt to bridge the limitations and extend the applicability of each technique. An important aspect in the multi-modal combination is the ability to reveal different contrast from each modality in order to reveal disease specific biomarkers. This however is not straightforward; the ability to combine multiple information collected from tissue in order to devise an approach with detection sensitivity and specificity is often confronted with limitations associated with the heterogeneity of disease from patient to patient or even within the same patient. While a large number of optical methods are geared towards detecting endogenous contrast (vascularization, hypoxia, auto-fluorescence, presence of lipids or NADH with CARS, 2PM, *etc.*), having the obvious advantage of not requiring injection of specific probes, the utilization of induced contrast, in particular contrast with biochemical or molecular specificity may prove an important parameter in improving diagnostics and theranostics in interventional procedures. For example, the emergence of 5-ALA fluorescence for glioma surgery[180] or the more recent use of a targeted fluorochrome agent in ovarian cancer surgery[204] are cases that combine biochemical/molecular contrast with wide field of view visualization capacity that can lead to practical implementations for enhancing interventional vision. Such methods can be further used to guide small field of view methods such as interventional CM or opto-acoustic imaging, in order to offer increased visualization capacities. Similarly, a promising alternative is the combination of macroscopic fluorescence imaging for biopsy guidance. Furthermore, 'dual modality' tumor targeted contrast agents are currently investigated[9,14,111,140,148] for the visualization of cancer with multiple modalities (MRI, PET, fluorescence) so that interventional imaging can be combined with pre-operative imaging.

Even though wide-field fluorescence imaging appears straightforward to implement, the approach is still limited by photon scattering. The approach cannot visualize with the resolution of microscopy methods and the fluorescence intensity is affected by tissue optical properties. This can lead to false negatives and false positives, unless special care is given to normalize the images for the effects of optical property variation, for accurate "medical-grade" images. Quantitative (normalized) planar fluorescence imaging, implemented in real-time mode can provide instant feedback to the surgeon and importantly, directly relate to his surgical or endoscopic vision, offering a natural extension of imaging in the operating room. With the addition of disease targeted fluorescence probe, the clinical sensitivity and specificity of the technique can be improved beyond the metrics achieved when visualizing intrinsic contrast. This "engineered" contrast can lead to significant flexibility in identifying disease but also important anatomical features, such as nerves.

In some applications, such as imaging of the upper and lower gastrointestinal tract, modalities that can be included in an endoscopic probe present a clear advantage. Tumor detection by means of autofluorescence imaging, confocal endo-microscopy, NBI, two photon microscopy and optical coherence imaging is becoming more and more widely accepted as a more reliable diagnosis or surgical guidance tool and should ultimately replace, or at the very least compliment, classical WLE in selective applications. Relying on various contrast sources for each methods (be it endogenous or exogenous), they possess physical

characteristics (penetration depth, resolution, field of view) that make them also suitable to replace classical tissue sectioning methods, with which they also share the need of a healthy reference to give definitive medical information and avoid false positive and false negative results. In that respect, using a multimodal approach to combine data, ideally anatomical and functional, should provide the clinician with the right tool to make the right decisions at all times.

In addition, opto-acoustic imaging is emerging as a modality with multiple advantages since it can provide anatomical, physiological and molecular high-resolution images from several millimeters to centimeters deep in tissue. The combination with wide field-of-view methods and the use of multi-spectral illumination for biomarker quantification comes with significant potential for interventional application as well. It is also foreseen that integration of opto-acoustic imagers in endoscopic probes, similar to the one commercially available for ultrasonic applications, will soon be performing well enough to be a credible alternative to other endoscopic modalities.

In conclusion, a variety of optical imaging techniques have emerged with the potential to provide intra-operatively guidance for cancer surgery and trustable evaluation of tumor margins. Since the most common surgical 'modality' is the visual inspection of tissue, epi-illumination fluorescence imaging is perhaps the most straightforward way to enhance the surgeon's vision by providing contrast between malignant and benign tissue. Featuring various sources of intrinsic and extrinsic tissue contrast, optical modalities have shown great potential for the future. With the increasing development of endoscopic implementations and minimal invasive surgery approaches, advanced optical imaging technologies are expected to play an increasingly important role in the future with the promise to improve overall survival and quality of life.

REFERENCES

[1]Adams, K. E., J. C. Rasmussen, C. Darne, I. C. Tan, M. B. Aldrich, M. V. Marshall, C. E. Fife, E. A. Maus, L. A. Smith, R. Guilloid, S. Hoy, and E. M. Sevick-Muraca. Direct evidence of lymphatic function improvement after advanced pneumatic compression device treatment of lymphedema. *Biomed. Opt. Express* 1:114–125, 2010.

[2]Adler, A., H. Pohl, I. S. Papanikolaou, H. Abou-Rebyeh, G. Schachschal, W. Veltzke-Schlieker, A. C. Khalifa, E. Setka, M. Koch, B. Wiedenmann, and T. Rosch. A prospective randomised study on narrow-band imaging versus conventional colonoscopy for adenoma detection: does narrow-band imaging induce a learning effect? *Gut* 57:59–64, 2008.

[3]Aguirre, A. D., P. Hsiung, T. H. Ko, I. Hartl, and J. G. Fujimoto. High-resolution optical coherence microscopy for high-speed, in vivo cellular imaging. *Opt. Lett.* 28:2064–2066, 2003.

[4]Aguirre, A. D., J. Sawinski, S. W. Huang, C. Zhou, W. Denk, and J. G. Fujimoto. High speed optical coherence microscopy with autofocus adjustment and a miniaturized endoscopic imaging probe. *Opt. Express* 18:4222–4239, 2010.

[5]Alberini, J. L., V. Edeline, A. L. Giraudet, L. Champion, B. Paulmier, O. Madar, A. Poinsignon, D. Bellet, and A. P. Pecking. Single photon emission tomography/computed tomography (SPET/CT) and positron emission tomography/computed tomography (PET/CT) to image cancer. *J. Surg. Oncol.* 103:602–606, 2011.

[6]Ambrosi, C. M., N. Moazami, A. M. Rollins, and I. R. Efimov. Virtual histology of the human heart using optical coherence tomography. *J. Biomed. Opt.* 14:054002, 2009.

[7]Ammar, D. A., T. C. Lei, O. Masihzadeh, E. A. Gibson, and M. Y. Kahook. Trans-scleral imaging of the human trabecular meshwork by two-photon microscopy. *Mol. Vis.* 17:583–590, 2011.

[8]Arens, C., T. Dreyer, K. Malzahn, and H. Glanz. Direct and indirect autofluorescence laryngoscopy in the diagnosis of laryngeal cancer and its precursor lesions. *Otolaryngol. Pol.* 58:197–203, 2004.

[9]Azhdarinia, A., N. Wilganowski, H. Robinson, P. Ghosh, S. Kwon, Z. W. Lazard, A. R. Davis, E. Olmsted-Davis, and E. M. Sevick-Muraca. Characterization of chemical, radiochemical and optical properties of a dual-labeled MMP-9 targeting peptide. *Bioorg. Med. Chem.* 19:3769–3776, 2011.

[10]Azzolini, C., F. Patelli, M. Codenotti, L. Pierro, and R. Brancato. Optical coherence tomography in idiopathic epiretinal macular membrane surgery. *Eur. J. Ophthalmol.* 9:206–211, 1999.

[11]Bandettini, P. Functional MRI today. *Int. J. Psychophysiol.* 63:138–145, 2007.

[12]Bassi, A., D. Brida, C. D'Andrea, G. Valentini, R. Cubeddu, S. De Silvestri, and G. Cerullo. Time-gated optical projection tomography. *Opt. Lett.* 35:2732–2734, 2010.

[13]Basu, S., T. C. Kwee, S. Surti, E. A. Akin, D. Yoo, and A. Alavi. Fundamentals of PET and PET/CT imaging. *Ann. N. Y. Acad. Sci.* 1228:1–18, 2011.

[14]Biswas, S., X. Wang, A. R. Morales, H. Y. Ahn, and K. D. Belfield. Integrin-targeting block copolymer probes for two-photon fluorescence bioimaging. *Biomacromolecules* 12:441–449, 2011.

[15]Bogaards, A., M. C. G. Aalders, C. C. Zeyl, S. de Blok, C. Dannecker, P. Hillemanns, H. Stepp, and H. J. C. M. Sterenborg. Localization and staging of cervical intraepithelial neoplasia using double ratio fluorescence imaging. *J. Biomed. Opt.* 7:215–220, 2002.

[16]Bogaards, A., H. J. Sterenborg, J. Trachtenberg, B. C. Wilson, and L. Lilge. In vivo quantification of fluorescent molecular markers in real-time by ratio imaging for diagnostic screening and image-guided surgery. *Lasers Surg. Med.* 39:605–613, 2007.

[17]Bottiroli, G., A. C. Croce, D. Locatelli, R. Nano, E. Giombelli, A. Messina, and E. Benericetti. Brain tissue autofluorescence: an aid for intraoperative delineation of tumor resection margins. *Cancer Detect. Prev.* 22:330–339, 1998.

[18]Bradley, R. S., and M. S. Thorniley. A review of attenuation correction techniques for tissue fluorescence. *J. R. Soc. Interface* 3:1–13, 2006.
[19]Brown, E. N., N. S. Burris, J. Gu, Z. N. Kon, P. Laird, S. Kallam, C. M. Tang, J. M. Schmitt, and R. S. Poston. Thinking inside the graft: applications of optical coherence tomography in coronary artery bypass grafting. *J. Biomed. Opt*. 12:051704, 2007.
[20]Buckler, A. J., J. L. Mulshine, R. Gottlieb, B. S. Zhao, P. D. Mozley, and L. Schwartz. The use of volumetric CT as an imaging biomarker in lung cancer. *Acad. Radiol*. 17:100–106, 2010.
[21]Buehler, A., E. Herzog, D. Razansky, and V. Ntziachristos. Video rate optoacoustic tomography of mouse kidney perfusion. *Opt. Lett*. 35:2475–2477, 2010.
[22]Burns, J. A., K. H. Kim, J. F. deBoer, R. R. Anderson, and S. M. Zeitels. Polarization-sensitive optical coherence tomography imaging of benign and malignant laryngeal lesions: an in vivo study. *Otolaryngol. Head Neck Surg*. 145:91–99, 2011.
[23]Capelle, L. G., J. Haringsma, A. C. de Vries, E. W. Steyerberg, K. Biermann, H. van Dekken, and E. J. Kuipers. Narrow band imaging for the detection of gastric intestinal metaplasia and dysplasia during surveillance endoscopy. *Dig. Dis. Sci*. 55:3442–3448, 2010.
[24]Carlson, A. L., A. M. Gillenwater, M. D. Williams, A. K. El-Naggar, and R. R. Richards-Kortum. Confocal microscopy and molecular-specific optical contrast agents for the detection of oral neoplasia. *Technol. Cancer Res. Treat*. 6:361–374, 2007.
[25]Chen, S. D., J. F. Salmon, and C. K. Patel. Videoendoscope-guided fluorescein-assisted vitrectomy for phakic malignant glaucoma. *Arch. Ophthalmol*. 123:1419–1421, 2005.
[26]Cherry, S. R. Multimodality imaging: beyond PET/CT and SPECT/CT. *Semin. Nucl. Med*. 39:348–353, 2009.
[27]Choi, W. I., J. Y. Kim, C. Kang, C. C. Byeon, Y. H. Kim, and G. Tae. Tumor regression in vivo by photothermal therapy based on gold-nanorod-loaded, functional nanocarriers. *ACS Nano* 5:1995–2003, 2011.
[28]Choi, W. J., I. Jeon do, S. G. Ahn, J. H. Yoon, S. Kim, and B. H. Lee. Full-field optical coherence microscopy for identifying live cancer cells by quantitative measurement of refractive index distribution. *Opt. Express* 18:23285–23295, 2010.
[29]Cicchi, R., and F. S. Pavone. Non-linear fluorescence lifetime imaging of biological tissues. *Anal. Bioanal. Chem*. 400:2687–2697, 2011.
[30]Collier, T., M. Guillaud, M. Follen, A. Malpica, and R. Richards-Kortum. Real-time reflectance confocal microscopy: comparison of two-dimensional images and three-dimensional image stacks for detection of cervical precancer. *J. Biomed. Opt*. 12:024021, 2007.
[31]Conovaloff, A., H. W. Wang, J. X. Cheng, and A. Panitch. Imaging growth of neurites in conditioned hydrogel by coherent anti-stokes raman scattering microscopy. *Organogenesis* 5:231–237, 2009.
[32]Conti, M. Focus on time-of-flight PET: the benefits of improved time resolution. *Eur. J. Nucl. Med. Mol. Imaging* 38:1147–1157, 2011.
[33]Crane, L. M., G. Themelis, H. J. Arts, K. T. Buddingh, A. H. Brouwers, V. Ntziachristos, G. M. van Dam, and A. G. van der Zee. Intraoperative near-infrared fluorescence imaging for sentinel lymph node detection in vulvar cancer: first clinical results. *Gynecol. Oncol*. 120:291–295, 2011.
[34]Crane, L. M., G. Themelis, R. G. Pleijhuis, N. J. Harlaar, A. Sarantopoulos, H. J. Arts, A. G. van der Zee, N. Vasilis, and G. M. van Dam. Intraoperative multispectral fluorescence imaging for the detection of the sentinel lymph node in cervical cancer: a novel concept. *Mol. Imaging Biol*. 13:1043–1049, 2010.
[35]Curvers, W., L. Baak, R. Kiesslich, A. Van Oijen, T. Rabenstein, K. Ragunath, J. F. Rey, P. Scholten, U. Seitz, F. Ten Kate, P. Fockens, and J. Bergman. Chromoendoscopy and narrow-band imaging compared with high-resolution magnification endoscopy in Barrett's esophagus. *Gastroenterology* 134:670–679, 2008.
[36]Curvers, W. L., C. J. Bohmer, R. C. Mallant-Hent, A. H. Naber, C. I. Ponsioen, K. Ragunath, R. Singh, M. B. Wallace, H. C. Wolfsen, L. M. Song, R. Lindeboom, P. Fockens, and J. J. Bergman. Mucosal morphology in Barrett's esophagus: interobserver agreement and role of narrow band imaging. *Endoscopy* 40:799–805, 2008.
[37]Curvers, W. L., R. Singh, L. M. Song, H. C. Wolfsen, K. Ragunath, K. Wang, M. B. Wallace, P. Fockens, and J. J. Bergman. Endoscopic tri-modal imaging for detection of early neoplasia in Barrett's oesophagus: a multi-centre feasibility study using high-resolution endoscopy, autofluorescence imaging and narrow band imaging incorporated in one endoscopy system. *Gut* 57:167–172, 2008.
[38]De Veld, D. C., M. J. Witjes, H. J. Sterenborg, and J. L. Roodenburg. The status of in vivo autofluorescence spectroscopy and imaging for oral oncology. *Oral Oncol*. 41:117–131, 2005.
[39]Desai, N. D., S. Miwa, D. Kodama, T. Koyama, G. Cohen, M. P. Pelletier, E. A. Cohen, G. T. Christakis, B. S. Goldman, and S. E. Fremes. A randomized comparison of intraoperative indocyanine green angiography and transit-time flow measurement to detect technical errors in coronary bypass grafts. *J. Thorac. Cardiovasc. Surg*. 132:585–594, 2006.
[40]Detre, J. A. Clinical applicability of functional MRI. *J. Magn. Reson. Imaging JMRI* 23:808–815, 2006.
[41]Dima, A., and V. Ntziachristos. Optoacoustic imaging for clinical applications: devices and methods. *Expert Opin. Med. Diagn*. 5:263–272, 2011.
[42]Drezek, R., C. Brookner, I. Pavlova, I. Boiko, A. Malpica, R. Lotan, M. Follen, and R. Richards-Kortum. Autofluorescence microscopy of fresh cervical-tissue sections reveals alterations in tissue biochemistry with dysplasia. *Photochem. Photobiol*. 73:636–641, 2001.
[43]Dunn, J., and L. Lovat. Photodynamic therapy using 5-aminolaevulinic acid for the treatment of dysplsia in Barrett's oesophagus. *Expert Opin. Pharmacol*. 9:851–858, 2008.
[44]Durr, N. J., C. T. Weisspfennig, B. A. Holfeld, and A. Ben-Yakar. Maximum imaging depth of two-photon autofluorescence microscopy in epithelial tissues. *J. Biomed. Opt*. 16:026008, 2011.
[45]Duyn, J. H. Study of brain anatomy with high-field MRI: recent progress. *Magn. Reson. Imaging* 28:1210–1215, 2010.
[46]East, J. E., N. Suzuki, M. Stavrinidis, T. Guenther, H. J. Thomas, and B. P. Saunders. Narrow band imaging for colonoscopic surveillance in hereditary non-polyposis colorectal cancer. *Gut* 57:65–70, 2008.
[47]Ericson, M. B., C. Simonsson, S. Guldbrand, C. Ljungblad, J. Paoli, and M. Smedh. Two-photon laser-scanning fluorescence microscopy applied for studies of human skin. *J. Biophotonics* 1:320–330, 2008.

[48]Erie, J. C., J. W. McLaren, and S. V. Patel. Confocal microscopy in ophthalmology. *Am. J. Ophthalmol.* 148:639–646, 2009.
[49]Evans, C. L., E. O. Potma, M. Puoris'haag, D. Cote, C. P. Lin, and X. S. Xie. Chemical imaging of tissue in vivo with video-rate coherent anti-Stokes Raman scattering microscopy. *Proc. Natl. Acad. Sci. USA* 102:16807–16812, 2005.
[50]Evans, C. L., X. Xu, S. Kesari, X. S. Xie, S. T. Wong, and G. S. Young. Chemically-selective imaging of brain structures with CARS microscopy. *Opt. Express* 15:12076–12087, 2007.
[51]Evans, J. A., J. M. Poneros, B. E. Bouma, J. Bressner, E. F. Halpern, M. Shishkov, G. Y. Lauwers, M. Mino-Kenudson, N. S. Nishioka, and G. J. Tearney. Optical coherence tomography to identify intramucosal carcinoma and high-grade dysplasia in Barrett's esophagus. *Clin. Gastroenterol. Hepatol.* 4:38–43, 2006.
[52]Ewelt, C., F. W. Floeth, J. Felsberg, H. J. Steiger, M. Sabel, K. J. Langen, G. Stoffels, and W. Stummer. Finding the anaplastic focus in diffuse gliomas: the value of Gd-DTPA enhanced MRI, FET-PET, and intraoperative. ALA-derived tissue fluorescence. *Clin. Neurol. Neurosurg.* 113:541–547, 2011.
[53]Fayter, D., M. Corbett, M. Heirs, D. Fox, and A. Eastwood. A systematic review of photodynamic therapy in the treatment of pre-cancerous skin conditions, Barrett's oesophagus and cancers of the biliary tract, brain, head and neck, lung, oesophagus and skin. *Health Technol. Assess.* 14:1–288, 2010.
[54]Ferris, D. G., R. A. Lawhead, E. D. Dickman, N. Holtzapple, J. A. Miller, S. Grogan, S. Bambot, A. Agrawal, and M. L. Faupel. Multimodal hyperspectral imaging for the noninvasive diagnosis of cervical neoplasia. *J. Low Genit. Tract Dis.* 5:65–72, 2001.
[55]Filip, M., S. Iordache, A. Săftoiu, and T. Ciurea. Autofluorescence imaging and magnification endoscopy. *World J. Gastroenterol.* 17:9–14, 2011.
[56]Fu, Y., T. B. Huff, H. W. Wang, H. Wang, and J. X. Cheng. Ex vivo and in vivo imaging of myelin fibers in mouse brain by coherent anti-Stokes Raman scattering microscopy. *Opt. Express* 16:19396–19409, 2008.
[57]Gallego-Pinazo, R., A. M. Suelves-Cogollos, R. Dolz-Marco, J. F. Arevalo, S. Garcia-Delpech, J. L. Mullor, and M. Diaz-Llopis. Macular laser photocoagulation guided by spectral-domain optical coherence tomography versus fluorescein angiography for diabetic macular edema. *Clin. Ophthalmol.* 5:613–617, 2011.
[58]Gallwas, J. K., L. Turk, H. Stepp, S. Mueller, R. Ochsenkuehn, K. Friese, and C. Dannecker. Optical coherence tomography for the diagnosis of cervical intraepithelial neoplasia. *Lasers Surg. Med.* 43:206–212, 2011.
[59]Gambichler, T., G. Moussa, and P. Altmeyer. A pilot study of fluorescence diagnosis of basal cell carcinoma using a digital flash light based imaging system. *Photodermatol. Photoimmunol. Photomed.* 24:67–71, 2008.
[60]Gao, L., H. Zhou, M. J. Thrall, F. Li, Y. Yang, Z. Wang, P. Luo, K. K. Wong, G. S. Palapattu, and S. T. Wong. Label-free high-resolution imaging of prostate glands and cavernous nerves using coherent anti-Stokes Raman scattering microscopy. *Biomed. Opt. Express* 2:915–926, 2011.
[61]Garcia-Garcia, H. M., M. A. Costa, and P. W. Serruys. Imaging of coronary atherosclerosis: intravascular ultrasound. *Eur. Heart J.* 31:2456–2469, 2010.
[62]Gareau, D. S., Y. Li, B. Huang, Z. Eastman, K. S. Nehal, and M. Rajadhyaksha. Confocal mosaicing microscopy in Mohs skin excisions: feasibility of rapid surgical pathology. *J. Biomed. Opt.* 13:054001, 2008.
[63]Georgakoudi, I., B. C. Jacobson, M. G. Muller, E. E. Sheets, K. Badizadegan, D. L. Carr-Locke, C. P. Crum, C. W. Boone, R. R. Dasari, J. Van Dam, and M. S. Feld. NAD(P)H and collagen as in vivo quantitative fluorescent biomarkers of epithelial precancerous changes. *Cancer Res.* 62:682–687, 2002.
[64]Gluckman, J. L., and R. P. Zitsch. Photodynamic therapy in the management of head and neck cancer. *Cancer Treat. Res.* 52:95–113, 1990.
[65]Goo, H. W. State-of-the-art CT imaging techniques for congenital heart disease. *Korean J. Radiol.* 11:4–18, 2010.
[66]Gotoh, K., T. Yamada, O. Ishikawa, H. Takahashi, H. Eguchi, M. Yano, H. Ohigashi, Y. Tomita, Y. Miyamoto, and S. Imaoka. A novel image-guided surgery of hepatocellular carcinoma by indocyanine green fluorescence imaging navigation. *J. Surg. Oncol.* 100:75–79, 2009.
[67]Grimwood, A., L. Garcia, J. Bamber, J. Holmes, P. Woolliams, P. Tomlins, and Q. A. Pankhurst. Elastographic contrast generation in optical coherence tomography from a localized shear stress. *Phys. Med. Biol.* 55:5515–5528, 2010.
[68]Grosberg, L. E., A. J. Radosevich, S. Asfaha, T. C. Wang, and E. M. Hillman. Spectral characterization and unmixing of intrinsic contrast in intact normal and diseased gastric tissues using hyperspectral two-photon microscopy. *PLoS one* 6:e19925, 2011.
[69]Guldbrand, S., C. Simonsson, M. Goksor, M. Smedh, and M. B. Ericson. Two-photon fluorescence correlation microscopy combined with measurements of point spread function; investigations made in human skin. *Opt. Express* 18:15289–15302, 2010.
[70]Haglund, M. M., M. S. Berger, and D. W. Hochman. Enhanced optical imaging of human gliomas and tumor margins. *Neurosurgery* 38:308–317, 1996.
[71]Haka, A. S., Z. Volynskaya, J. A. Gardecki, J. Nazemi, R. Shenk, N. Wang, R. R. Dasari, M. Fitzmaurice, and M. S. Feld. Diagnosing breast cancer using Raman spectroscopy: prospective analysis. *J. Biomed. Opt.* 14:054023, 2009.
[72]Hanaoka, N., N. Uedo, A. Shiotani, T. Inoue, Y. Takeuchi, K. Higashino, R. Ishihara, H. Iishi, K. Haruma, and M. Tatsuta. Autofluorescence imaging for predicting development of metachronous gastric cancer after *Helicobacter pylori* eradication. *J. Gastroenterol. Hepatol.* 25:1844–1849, 2010.
[73]Handa, T., R. G. Katare, H. Nishimori, S. Wariishi, T. Fukutomi, M. Yamamoto, S. Sasaguri, and T. Sato. New device for intraoperative graft assessment: HyperEye charge-coupled device camera system. *Gen. Thorac. Cardiovasc. Surg.* 58:68–77, 2010.
[74]Hassan, M., J. Riley, V. Chernomordik, P. Smith, R. Pursley, S. B. Lee, J. Capala, and A. H. Gandjbakhche. Fluorescence lifetime imaging system for in vivo studies. *Mol. Imaging* 6:229–236, 2007.
[75]Haxel, B. R., M. Goetz, R. Kiesslich, and J. Gosepath. Confocal endomicroscopy: a novel application for imaging of oral and oropharyngeal mucosa in human. *Eur. Arch. Otorhinolaryngol.* 267:443–448, 2010.
[76]Helmchen, F., and W. Denk. Deep tissue two-photon microscopy. *Nat. Methods* 2:932–940, 2005.
[77]Hinz, T., L. K. Ehler, H. Voth, I. Fortmeier, T. Hoeller, T. Hornung, and M. H. Schmid-Wendtner. Assessment of

tumor thickness in melanocytic skin lesions: comparison of optical coherence tomography, 20-MHz ultrasound and histopathology. *Dermatology* 223:161–168, 2011.
[78]Holm, C., M. Mayr, E. Hofter, A. Becker, U. J. Pfeiffer, and W. Muhlbauer. Intraoperative evaluation of skin-flap viability using laser-induced fluorescence of indocyanine green. *Br. J. Plast. Surg.* 55:635–644, 2002.
[79]Holmes, J. OCT technology development: where are we now? A commercial perspective. *J. Biophotonics* 2:347–352, 2009.
[80]Horky, L. L. and S. T. Treves. PET and SPECT in brain tumors and epilepsy. *Neurosurg. Clinics N. Am.* 22:169–184, viii, 2011.
[81]Hu, S., K. Maslov, and L. V. Wang. Noninvasive label-free imaging of microhemodynamics by optical-resolution photoacoustic microscopy. *Opt. Express* 17:7688–7693, 2009.
[82]Hu, S., and L. V. Wang. Photoacoustic imaging and characterization of the microvasculature. *J. Biomed. Opt.* 15:011101, 2010.
[83]Huber, M. A. Assessment of the VELscope as an adjunctive examination tool. *Tex Dent. J.* 126:528–535, 2009.
[84]Huh, W. K., R. M. Cestero, F. A. Garcia, M. A. Gold, R. S. Guido, K. McIntyre-Seltman, D. M. Harper, L. Burke, S. T. Sum, R. F. Flewelling, and R. D. Alvarez. Optical detection of high-grade cervical intraepithelial neoplasia in vivo: results of a 604-patient study. *Am. J. Obstet. Gynecol.* 190:1249–1257, 2004.
[85]Hungerhuber, E., H. Stepp, M. Kriegmair, C. Stief, A. Hofstetter, A. Hartmann, R. Knuechel, A. Karl, S. Tritschler, and D. Zaak. Seven years' experience with 5-aminolevulinic acid in detection of transitional cell carcinoma of the bladder. *Urology* 69:260–264, 2007.
[86]Ikematsu, H., T. Matsuda, F. Emura, Y. Saito, T. Uraoka, K. I. Fu, K. Kaneko, A. Ochiai, T. Fujimori, and Y. Sano. Efficacy of capillary pattern type IIIA/IIIB by magnifying narrow band imaging for estimating depth of invasion of early colorectal neoplasms. *BMC Gastroenterol.* 10:33, 2010.
[87]Ikematsu, H., Y. Saito, and H. Yamano. Comparative evaluation of endoscopic factors from conventional colonoscopy and narrow-band imaging of colorectal lesions. *Dig. Endosc.* 23(Suppl 1):95–100, 2011.
[88]Inoue, K., N. Wakabayashi, Y. Morimoto, K. Miyawaki, A. Kashiwa, N. Yoshida, K. Nakano, H. Takada, Y. Harada, N. Yagi, Y. Naito, T. Takamatsu, and T. Yoshikawa. Evaluation of autofluorescence colonoscopy for diagnosis of superficial colorectal neoplastic lesions. *Int. J. Colorectal Dis.* 25:811–816, 2010.
[89]Ishizawa, T., N. Fukushima, J. Shibahara, K. Masuda, S. Tamura, T. Aoki, K. Hasegawa, Y. Beck, M. Fukayama, and N. Kokudo. Real-time identification of liver cancers by using indocyanine green fluorescent imaging. *Cancer* 115:2491–2504, 2009.
[90]Jayaprakash, V., M. Sullivan, M. Merzianu, N. R. Rigual, T. R. Loree, S. R. Popat, K. B. Moysich, S. Ramananda, T. Johnson, J. R. Marshall, A. D. Hutson, T. S. Mang, B. C. Wilson, S. R. Gill, J. Frustino, A. Bogaards, and M. E. Reid. Autofluorescence-guided surveillance for oral cancer. *Cancer Prev. Res. (Phila)* 2:966–974, 2009.
[91]Jerjes, W., T. Upile, S. Akram, and C. Hopper. The surgical palliation of advanced head and neck cancer using photodynamic therapy. *Clin. Oncol.* 22:785–791, 2010.
[92]Jiang, X., J. Zhong, Y. Liu, H. Yu, S. Zhuo, and J. Chen. Two-photon fluorescence and second-harmonic generation imaging of collagen in human tissue based on multiphoton microscopy. *Scanning* 33:53–56, 2011.
[93]Jocham, D., F. Witjes, S. Wagner, B. Zeylemaker, J. van Moorselaar, M. O. Grimm, R. Muschter, G. Popken, F. Konig, and R. Knuchel. Improved detection and treatment of bladder cancer using hexaminolevulinate imaging: a prospective, phase III multicenter study. *J. Urol.* 174:862–866, 2005.
[94]Johansson, A., J. Axelsson, S. Andersson-Engels, and J. Swartling. Realtime light dosimetry software tools for interstitial photodynamic therapy of the human prostate. *Med. Phys.* 34:4309–4321, 2007.
[95]Jose, J., S. Manohar, R. G. Kolkman, W. Steenbergen, and T. G. van Leeuwen. Imaging of tumor vasculature using Twente photoacoustic systems. *J. Biophotonics* 2:701–717, 2009.
[96]Kara, M. A., M. Ennahachi, P. Fockens, F. J. ten Kate, and J. J. Bergman. Detection and classification of the mucosal and vascular patterns (mucosal morphology) in Barrett's esophagus by using narrow band imaging. *Gastrointest. Endosc.* 64:155–166, 2006.
[97]Kara, M. A., F. P. Peters, P. Fockens, F. J. ten Kate, and J. J. Bergman. Endoscopic video-autofluorescence imaging followed by narrow band imaging for detecting early neoplasia in Barrett's esophagus. *Gastrointest. Endosc.* 64:176–185, 2006.
[98]Kato, M., M. Kaise, J. Yonezawa, H. Toyoizumi, N. Yoshimura, Y. Yoshida, M. Kawamura, and H. Tajiri. Magnifying endoscopy with narrow-band imaging achieves superior accuracy in the differential diagnosis of superficial gastric lesions identified with white-light endoscopy: a prospective study. *Gastrointest. Endosc.* 72:523–529, 2010.
[99]Kawakami, N., and A. Flugel. Knocking at the brain's door: intravital two-photon imaging of autoreactive T cell interactions with CNS structures. *Semin. Immunopathol.* 32:275–287, 2010.
[100]Keereweer, S., J. D. Kerrebijn, P. B. van Driel, B. Xie, E. L. Kaijzel, T. J. Snoeks, I. Que, M. Hutteman, J. R. van der Vorst, J. S. Mieog, A. L. Vahrmeijer, C. J. van de Velde, R. J. Baatenburg de Jong, and C. W. Lowik. Optical image-guided surgery—where do we stand? *Mol. Imaging Biol.* 13(199–207):2011, 2011.
[101]Kelder, W., H. Nimura, N. Takahashi, N. Mitsumori, G. M. van Dam, and K. Yanaga. Sentinel node mapping with indocyanine green (ICG) and infrared ray detection in early gastric cancer: an accurate method that enables a limited lymphadenectomy. *Eur. J. Surg. Oncol.* 36:552–558, 2010.
[102]Kellner, U., S. Kellner, and S. Weinitz. Fundus autofluorescence (488 NM) and near-infrared autofluorescence (787 NM) visualize different retinal pigment epithelium alterations in patients with age-related macular degeneration. *Retina* 30:6–15, 2010.
[103]Kiesslich, R., L. Gossner, M. Goetz, A. Dahlmann, M. Vieth, M. Stolte, A. Hoffman, M. Jung, B. Nafe, P. R. Galle, and M. F. Neurath. In vivo histology of Barrett's esophagus and associated neoplasia by confocal laser endomicroscopy. *Clin. Gastroenterol. Hepatol.* 4:979–987, 2006.
[104]Kim, C., C. Favazza, and L. V. Wang. In vivo photoacoustic tomography of chemicals: high-resolution functional and molecular optical imaging at new depths. *Chem. Rev.* 110:2756–2782, 2010.
[105]Kim, D. Y., J. Fingler, J. S. Werner, D. M. Schwartz, S. E. Fraser, and R. J. Zawadzki. In vivo volumetric imaging of

human retinal circulation with phase-variance optical coherence tomography. *Biomed. Opt. Express* 2:1504–1513, 2011.
[106]Kim, K. H., J. A. Burns, J. J. Bernstein, G. N. Maguluri, B. H. Park, and J. F. de Boer. In vivo 3D human vocal fold imaging with polarization sensitive optical coherence tomography and a MEMS scanning catheter. *Opt. Express* 18:14644–14653, 2010.
[107]König, K., H. Breunig, R. Bückle, M. Kellner Höfer, M. Weinigel, E. Büttner, W. Sterry, and J. Lademann. Optical skin biopsies by clinical CARS and multiphoton fluorescence/SHG tomography. *Laser Phys. Lett.* 8:465–468, 2011.
[108]Konig, K., and I. Riemann. High-resolution multiphoton tomography of human skin with subcellular spatial resolution and picosecond time resolution. *J. Biomed. Opt.* 8:432–439, 2003.
[109]Konig, K., M. Speicher, R. Buckle, J. Reckfort, G. McKenzie, J. Welzel, M. J. Koehler, P. Elsner, and M. Kaatz. Clinical optical coherence tomography combined with multiphoton tomography of patients with skin diseases. *J. Biophotonics* 2:389–397, 2009.
[110]Korde, V. R., E. Liebmann, and J. K. Barton. Design of a handheld optical coherence microscopy endoscope. *J. Biomed. Opt.* 16:066018, 2011.
[111]Koyama, Y., V. S. Talanov, M. Bernardo, Y. Hama, C. A. Regino, M. W. Brechbiel, P. L. Choyke, and H. Kobayashi. A dendrimer-based nanosized contrast agent dual-labeled for magnetic resonance and optical fluorescence imaging to localize the sentinel lymph node in mice. *J. Magn. Reson. Imaging* 25:866–871, 2007.
[112]Kraft, M., C. S. Betz, A. Leunig, and C. Arens. Value of fluorescence endoscopy for the early diagnosis of laryngeal cancer and its precursor lesions. *Head Neck* 33:941–948, 2011.
[113]Kubota, K., J. Kita, M. Shimoda, K. Rokkaku, M. Kato, Y. Iso, and T. Sawada. Intraoperative assessment of reconstructed vessels in living-donor liver transplantation, using a novel fluorescence imaging technique. *J. Hepatobiliary Pancreat. Surg.* 13:100–104, 2006.
[114]Kuroiwa, T., Y. Kajimoto, and T. Ohta. Development of a fluorescein operative microscope for use during malignant glioma surgery: a technical note and preliminary report. *Surg. Neurol.* 50:41–48, 1998; discussion 48–49.
[115]Kwee, T. C., S. Basu, B. Saboury, V. Ambrosini, D. A. Torigian, and A. Alavi. A new dimension of FDG-PET interpretation: assessment of tumor biology. *Eur. J. Nucl. Med. Mol. Imaging* 38:1158–1170, 2011.
[116]Lam, S., T. Kennedy, M. Unger, Y. E. Miller, D. Gelmont, V. Rusch, B. Gipe, D. Howard, J. C. LeRiche, A. Coldman, and A. F. Gazdar. Localization of bronchial intraepithelial neoplastic lesions by fluorescence bronchoscopy. *Chest* 113:696–702, 1998.
[117]Lane, P. M., T. Gilhuly, P. Whitehead, H. Zeng, C. F. Poh, S. Ng, P. M. Williams, L. Zhang, M. P. Rosin, and C. E. MacAulay. Simple device for the direct visualization of oral-cavity tissue fluorescence. *J. Biomed. Opt.* 11:024006, 2006.
[118]Le Harzic, R., I. Riemann, M. Weinigel, K. Konig, and B. Messerschmidt. Rigid and high-numerical-aperture two-photon fluorescence endoscope. *Appl. Opt.* 48:3396–3400, 2009.
[119]Le, T. T., T. B. Huff, and J. X. Cheng. Coherent anti-Stokes Raman scattering imaging of lipids in cancer metastasis. *BMC Cancer* 9:42, 2009.
[120]Lee, K. S., K. P. Thompson, P. Meemon, and J. P. Rolland. Cellular resolution optical coherence microscopy with high acquisition speed for in vivo human skin volumetric imaging. *Opt. Lett.* 36:2221–2223, 2011.
[121]Lee, P., R. M. van den Berg, S. Lam, A. F. Gazdar, K. Grunberg, A. McWilliams, J. Leriche, P. E. Postmus, and T. G. Sutedja. Color fluorescence ratio for detection of bronchial dysplasia and carcinoma in situ. *Clin. Cancer Res.* 15:4700–4705, 2009.
[122]Leunig, A., C. S. Betz, M. Mehlmann, H. Stepp, S. Arbogast, G. Grevers, and R. Baumgartner. Detection of squamous cell carcinoma of the oral cavity by imaging 5-aminolevulinic acid-induced protoporphyrin IX fluorescence. *Laryngoscope* 110:78–83, 2000.
[123]Li, L., K. Maslov, G. Ku, and L. V. Wang. Three-dimensional combined photoacoustic and optical coherence microscopy for in vivo microcirculation studies. *Opt. Express* 17:16450–16455, 2009.
[124]Lim, L. G., M. Bajbouj, S. von Delius, and A. Meining. Fluorescein-enhanced autofluorescence imaging for accurate differentiation of neoplastic from non-neoplastic colorectal polyps: a feasibility study. *Endoscopy* 43:419–424, 2011.
[125]Lim, R. S., A. Kratzer, N. P. Barry, S. Miyazaki-Anzai, M. Miyazaki, W. W. Mantulin, M. Levi, E. O. Potma, and B. J. Tromberg. Multimodal CARS microscopy determination of the impact of diet on macrophage infiltration and lipid accumulation on plaque formation in ApoE-deficient mice. *J. Lipid Res.* 51:1729–1737, 2010.
[126]Lim, V. Y., L. Buellesfeld, and E. Grube. Images in cardiology. Optical coherence tomography imaging of thrombus protrusion through stent struts after stenting in acute coronary syndrome. *Heart* 92:409, 2006.
[127]Lopez, R. F. V., N. Lange, R. Guy, and M. V. L. B. Bentley. Photodynamic therapy of skin cancer: controlled drug delivery of 5-ALA and its esters. *Adv. Drug Deliv. Rev.* 56:77–94, 2004.
[128]Luck, B. L., K. D. Carlson, A. C. Bovik, and R. R. Richards-Kortum. An image model and segmentation algorithm for reflectance confocal images of in vivo cervical tissue. *IEEE Trans. Image Process* 14:1265–1276, 2005.
[129]Maitland, K. C., A. M. Gillenwater, M. D. Williams, A. K. El-Naggar, M. R. Descour, and R. R. Richards-Kortum. In vivo imaging of oral neoplasia using a miniaturized fiber optic confocal reflectance microscope. *Oral Oncol.* 44:1059–1066, 2008.
[130]Malmstrom, P. U., M. Grabe, E. S. Haug, P. Hellstrom, G. G. Hermann, K. Mogensen, M. Raitanen, and R. Wahlqvist. Role of hexaminolevulinate-guided fluorescence cystoscopy in bladder cancer: critical analysis of the latest data and European guidance. *Scand. J. Urol. Nephrol.*, 2011.
[131]Marschall, S., B. Sander, M. Mogensen, T. M. Jorgensen, and P. E. Andersen. Optical coherence tomography-current technology and applications in clinical and biomedical research. *Anal. Bioanal. Chem.* 400:2699–2720, 2011.
[132]Menard-Moyon, C., K. Kostarelos, M. Prato, and A. Bianco. Functionalized carbon nanotubes for probing and modulating molecular functions. *Chem. Biol.* 17:107–115, 2010.
[133]Miller, J. C., A. J. Fischman, S. L. Aquino, M. A. Blake, J. H. Thrall, and S. I. Lee. FDG-PET CT for tumor imaging. *J. Am. Coll. Radiol.* 4:256–259, 2007.
[134]Moghissi, K., K. Dixon, M. Stringer, and J. A. Thorpe. Photofrin PDT for early stage oesophageal cancer: long

term results in 40 patients and literature review. *Photodiagnosis Photodyn. Ther.* 6:159–166, 2009.
[135]Muller, M. G., T. A. Valdez, I. Georgakoudi, V. Backman, C. Fuentes, S. Kabani, N. Laver, Z. Wang, C. W. Boone, R. R. Dasari, S. M. Shapshay, and M. S. Feld. Spectroscopic detection and evaluation of morphologic and biochemical changes in early human oral carcinoma. *Cancer* 97:1681–1692, 2003.
[136]Nabavi, A., H. Thurm, B. Zountsas, T. Pietsch, H. Lanfermann, U. Pichlmeier, and M. Mehdorn. Five-aminolevulinic acid for fluorescence-guided resection of recurrent malignant gliomas: a phase ii study. *Neurosurgery* 65:1070–1076, 2009; discussion 1076–1077.
[137]Nakada, T. Clinical application of high and ultra high-field MRI. *Brain Dev.* 29:325–335, 2007.
[138]Nguyen, F. T., A. M. Zysk, J. G. Kotynek, F. J. Bellafiore, K. M. Rowland, P. A. Johnson, J. E. Chaney, and S. A. Boppart. Proceedings of SPIE 6430, 64300H.
[139]Nguyen, N. Q., A. V. Biankin, R. W. Leong, D. K. Chang, P. H. Cosman, P. Delaney, J. G. Kench, and N. D. Merrett. Real time intraoperative confocal laser microscopy-guided surgery. *Ann. Surg.* 249:735–737, 2009.
[140]Nguyen, Q. T., E. S. Olson, T. A. Aguilera, T. Jiang, M. Scadeng, L. G. Ellies, and R. Y. Tsien. Surgery with molecular fluorescence imaging using activatable cell-penetrating peptides decreases residual cancer and improves survival. *Proc. Natl. Acad. Sci. USA* 107:4317–4322, 2010.
[141]Niederhauser, J. J., M. Jaeger, R. Lemor, P. Weber, and M. Frenz. Combined ultrasound and optoacoustic system for real-time high-contrast vascular imaging in vivo. *IEEE Trans. Med. Imaging* 24:436–440, 2005.
[142]Nimsky, C., O. Ganslandt, B. von Keller, and R. Fahlbusch. Intraoperative high-field MRI: anatomical and functional imaging. *Acta Neurochir. Suppl.* 98:87–95, 2006.
[143]Noppen, M., G. Stratakos, S. Verbanck, J. D'Haese, M. Meysman, and W. Vincken. Fluorescein-enhanced autofluorescence thoracoscopy in primary spontaneous pneumothorax. *Am. J. Respir. Crit. Care Med.* 170:680–682, 2004.
[144]Ntziachristos, V. Going deeper than microscopy: the optical imaging frontier in biology. *Nat. Meth.* 7:603–614, 2010.
[145]Ntziachristos, V., and D. Razansky. Molecular imaging by means of multispectral optoacoustic tomography (MSOT). *Chem. Rev.* 110:2783–2794, 2010.
[146]Ntziachristos, V., G. Turner, J. Dunham, S. Windsor, A. Soubret, J. Ripoll, and H. A. Shih. Planar fluorescence imaging using normalized data. *J. Biomed. Opt.* 10:064007, 2005.
[147]Ntziachristos, V., A. G. Yodh, M. Schnall, and B. Chance. Concurrent MRI and diffuse optical tomography of breast after indocyanine green enhancement. *Proc. Natl. Acad. Sci. USA* 97:2767–2772, 2000.
[148]Ogawa, M., C. A. Regino, J. Seidel, M. V. Green, W. Xi, M. Williams, N. Kosaka, P. L. Choyke, and H. Kobayashi. Dual-modality molecular imaging using antibodies labeled with activatable fluorescence and a radionuclide for specific and quantitative targeted cancer detection. *Bioconjug. Chem.* 20:2177–2184, 2009.
[149]Orrison, Jr., W. W., K. V. Snyder, L. N. Hopkins, C. J. Roach, E. N. Ringdahl, R. Nazir, and E. H. Hanson. Whole-brain dynamic CT angiography and perfusion imaging. *Clin. Radiol.* 66:566–574, 2011.
[150]Parekh, S. H., Y. J. Lee, K. A. Aamer, and M. T. Cicerone. Label-free cellular imaging by broadband coherent anti-Stokes Raman scattering microscopy. *Biophys. J.* 99:2695–2704, 2010.
[151]Pedrosa, M. C., B. A. Barth, D. J. Desilets, V. Kaul, S. R. Kethu, P. R. Pfau, J. L. Tokar, S. Varadarajulu, A. Wang, L. M. Wong Kee Song, and S. A. Rodriguez. Enhanced ultrasound imaging. *Gastrointest. Endosc.* 73:857–860, 2011.
[152]Placantonakis, D. G., A. Tabaee, V. K. Anand, D. Hiltzik, and T. H. Schwartz. Safety of low-dose intrathecal fluorescein in endoscopic cranial base surgery. *Neurosurgery* 61:161–165, 2007; discussion 165–166.
[153]Pliss, A., A. N. Kuzmin, A. V. Kachynski, and P. N. Prasad. Biophotonic probing of macromolecular transformations during apoptosis. *Proc. Natl. Acad. Sci. USA* 107:12771–12776, 2010.
[154]Pohl, H., T. Rosch, M. Vieth, M. Koch, V. Becker, M. Anders, A. C. Khalifa, and A. Meining. Miniprobe confocal laser microscopy for the detection of invisible neoplasia in patients with Barrett's oesophagus. *Gut* 57: 1648–1653, 2008.
[155]Pysz, M. A., and J. K. Willmann. Targeted contrast-enhanced ultrasound: an emerging technology in abdominal and pelvic imaging. *Gastroenterology* 140:785–790, 2011.
[156]Reimers, B., D. Nikas, E. Stabile, L. Favero, S. Sacca, A. Cremonesi, and P. Rubino. Preliminary experience with optical coherence tomography imaging to evaluate carotid artery stents: safety, feasibility and techniques. *EuroIntervention* 7:98–105, 2011.
[157]Rex, D. K., and C. C. Helbig. High yields of small and flat adenomas with high-definition colonoscopes using either white light or narrow band imaging. *Gastroenterology* 133:42–47, 2007.
[158]Rice, W. L., D. L. Kaplan, and I. Georgakoudi. Two-photon microscopy for non-invasive, quantitative monitoring of stem cell differentiation. *PLoS one* 5:e10075, 2010.
[159]Rimpiläinen, R., N. Hautala, J. Koskenkari, J. Rimpiläinen, P. Ohtonen, P. Mustonen, H. Surcel, E. Savolainen, M. Mosorin, and T. Ala-Kokko. Comparison of use of minimized cardiopulmonary bypass with conventional techniques on the incidence of retinal microemboli during aortic valve replacement surgery. *Perfusion* 26:479–486, 2011.
[160]Ris, H. B., T. Krueger, A. Giger, C. K. Lim, J. C. Stewart, U. Althaus, and H. J. Altermatt. Photodynamic therapy with mTHPC and polyethylene glycol-derived mTHPC: a comparative study on human tumour xenografts. *Br. J. Cancer* 79:1061–1066, 1999.
[161]Roblyer, D., R. Richards-Kortum, K. Sokolov, A. K. El-Naggar, M. D. Williams, C. Kurachi, and A. M. Gillenwater. Multispectral optical imaging device for in vivo detection of oral neoplasia. *J. Biomed. Opt.* 13:024019, 2008.
[162]Rogart, J. N., J. Nagata, C. S. Loeser, R. D. Roorda, H. Aslanian, M. E. Robert, W. R. Zipfel, and M. H. Nathanson. Multiphoton imaging can be used for microscopic examination of intact human gastrointestinal mucosa ex vivo. *Clin. Gastroenterol. Hepatol.* 6:95–101, 2008.
[163]Saftoiu, A. State-of-the-art imaging techniques in endoscopic ultrasound. *World J. Gastroenterol.* 17:691–696, 2011.
[164]Sahoo, N. G., H. Bao, Y. Pan, M. Pal, M. Kakran, H. K. Cheng, L. Li, and L. P. Tan. Functionalized carbon nanomaterials as nanocarriers for loading and delivery of a poorly water-soluble anticancer drug: a comparative study. *Chem Commun. (Camb.)* 47:5235–5237, 2011.

[165]Sanai, N., L. A. Snyder, N. J. Honea, S. W. Coons, J. M. Eschbacher, K. A. Smith, and R. F. Spetzler. Intraoperative confocal microscopy in the visualization of 5-aminolevulinic acid fluorescence in low-grade gliomas. *J. Neurosurg*. 115:740–748, 2011.
[166]Sandberg, C., J. Paoli, M. Gillstedt, C. B. Halldin, O. Larko, A. M. Wennberg, and M. B. Ericson. Fluorescence diagnostics of basal cell carcinomas comparing methyl-aminolaevulinate and aminolaevulinic acid and correlation with visual clinical tumour size. *Acta Derm. Venereol*. 91:398–403, 2011.
[167]Scepanovic, O. R., M. Fitzmaurice, A. Miller, C. R. Kong, Z. Volynskaya, R. R. Dasari, J. R. Kramer, and M. S. Feld. Multimodal spectroscopy detects features of vulnerable atherosclerotic plaque. *J. Biomed. Opt*. 16:011009, 2011.
[168]Schaafsma, B. E., J. S. D. Mieog, M. Hutteman, J. R. van der Vorst, P. J. K. Kuppen, C. W. G. M. Löwik, J. V. Frangioni, C. J. H. van de Velde, and A. L. Vahrmeijer. The clinical use of indocyanine green as a near infrared fluorescent contrast agent for image guided oncologic surgery. *J. Surg. Oncol*. 104(3):323–332, 2011.
[169]Scherschel, J. A., and M. Rubart. Cardiovascular imaging using two-photon microscopy. *Microsc. Microanal*. 14:492–506, 2008.
[170]Schwarz, R. A., W. Gao, C. Redden Weber, C. Kurachi, J. J. Lee, A. K. El-Naggar, R. Richards-Kortum, and A. M. Gillenwater. Noninvasive evaluation of oral lesions using depth-sensitive optical spectroscopy. *Cancer* 115:1669–1679, 2009.
[171]Schwarz, R. A., W. Gao, V. M. Stepanek, T. T. Le, V. S. Bhattar, M. D. Williams, J. K. Wu, N. Vigneswaran, K. Adler-Storthz, A. M. Gillenwater, and R. Richards-Kortum. Prospective evaluation of a portable depth-sensitive optical spectroscopy device to identify oral neoplasia. *Biomed. Opt. Express* 2:89–99, 2010.
[172]Sevick-Muraca, E. M., R. Sharma, J. C. Rasmussen, M. V. Marshall, J. A. Wendt, H. Q. Pham, E. Bonefas, J. P. Houston, L. Sampath, K. E. Adams, D. K. Blanchard, R. E. Fisher, S. B. Chiang, R. Elledge, and M. E. Mawad. Imaging of lymph flow in breast cancer patients after microdose administration of a near-infrared fluorophore: feasibility study. *Radiology* 246:734–741, 2008.
[173]Shakhov, A. V., A. B. Terentjeva, V. A. Kamensky, L. B. Snopova, V. M. Gelikonov, F. I. Feldchtein, and A. M. Sergeev. Optical coherence tomography monitoring for laser surgery of laryngeal carcinoma. *J. Surg. Oncol*. 77:253–258, 2001.
[174]Shao, X., W. Zheng, and Z. Huang. In vivo diagnosis of colonic precancer and cancer using near-infrared autofluorescence spectroscopy and biochemical modeling. *J. Biomed. Opt*. 16:067005, 2011.
[175]Shin, D., N. Vigneswaran, A. Gillenwater, and R. Richards-Kortum. Advances in fluorescence imaging techniques to detect oral cancer and its precursors. *Future Oncol*. 6:1143–1154, 2010.
[176]Shrestha, S., B. E. Applegate, J. Park, X. Xiao, P. Pande, and J. A. Jo. High-speed multispectral fluorescence lifetime imaging implementation for in vivo applications. *Opt. Lett*. 35:2558–2560, 2010.
[177]Spaide, R. F. Peripheral areas of nonperfusion in treated central retinal vein occlusion as imaged by wide-field fluorescein angiography. *Retina* 31:829–837, 2011.
[178]Standish, B. A., K. K. Lee, X. Jin, A. Mariampillai, N. R. Munce, M. F. Wood, B. C. Wilson, I. A. Vitkin, and V. X. Yang. Interstitial Doppler optical coherence tomography as a local tumor necrosis predictor in photodynamic therapy of prostatic carcinoma: an in vivo study. *Cancer Res*. 68:9987–9995, 2008.
[179]Steinkamp, J. A., and C. C. Stewart. Dual-laser, differential fluorescence correction method for reducing cellular background autofluorescence. *Cytometry* 7:566–574, 1986.
[180]Stockhammer, F., M. Misch, P. Horn, A. Koch, N. Fonyuy, and M. Plotkin. Association of F18-fluoro-ethyl-tyrosin uptake and 5-aminolevulinic acid-induced fluorescence in gliomas. *Acta Neurochir. (Wien)* 151:1377–1383, 2009.
[181]Stummer, W., U. Pichlmeier, T. Meinel, O. D. Wiestler, F. Zanella, and H. J. Reulen. Fluorescence-guided surgery with 5-aminolevulinic acid for resection of malignant glioma: a randomised controlled multicentre phase III trial. *Lancet Oncol*. 7:392–401, 2006.
[182]Sun, Y., J. Phipps, D. S. Elson, H. Stoy, S. Tinling, J. Meier, B. Poirier, F. S. Chuang, D. G. Farwell, and L. Marcu. Fluorescence lifetime imaging microscopy: in vivo application to diagnosis of oral carcinoma. *Opt. Lett*. 34:2081–2083, 2009.
[183]Svensson, T., S. Andersson-Engels, M. Einarsdottir, and K. Svanberg. In vivo optical characterization of human prostate tissue using near-infrared time-resolved spectroscopy. *J. Biomed. Opt*. 12:014022, 2007.
[184]Swartling, J., J. Axelsson, G. Ahlgren, K. M. Kalkner, S. Nilsson, S. Svanberg, K. Svanberg, and S. Andersson-Engels. System for interstitial photodynamic therapy with online dosimetry: first clinical experiences of prostate cancer. *J. Biomed. Opt*. 15:058003, 2010.
[185]Takahashi, M., T. Ishikawa, K. Higashidani, and H. Katoh. SPY: an innovative intra-operative imaging system to evaluate graft patency during off-pump coronary artery bypass grafting. *Interact. Cardiovasc. Thorac. Surg*. 3:479–483, 2004.
[186]Takeuchi, Y., N. Hanaoka, M. Hanafusa, R. Ishihara, K. Higashino, H. Iishi, and N. Uedo. Autofluorescence imaging of early colorectal cancer. *J. Biophotonics* 4:490–497, 2011.
[187]Tan, J., M. A. Quinn, J. M. Pyman, P. M. Delaney, and W. J. McLaren. Detection of cervical intraepithelial neoplasia in vivo using confocal endomicroscopy. *BJOG* 116:1663–1670, 2009.
[188]Tan, O., G. Li, A. T. Lu, R. Varma, and D. Huang. Mapping of macular substructures with optical coherence tomography for glaucoma diagnosis. *Ophthalmology* 115:949–956, 2008.
[189]Tanaka, A., K. Shimada, G. J. Tearney, H. Kitabata, H. Taguchi, S. Fukuda, M. Kashiwagi, T. Kubo, S. Takarada, K. Hirata, M. Mizukoshi, J. Yoshikawa, B. E. Bouma, and T. Akasaka. Conformational change in coronary artery structure assessed by optical coherence tomography in patients with vasospastic angina. *J. Am. Coll. Cardiol*. 58:1608–1613, 2011.
[190]Telenkov, S. A., D. P. Dave, S. Sethuraman, T. Akkin, and T. E. Milner. Differential phase optical coherence probe for depth-resolved detection of photothermal response in tissue. *Phys. Med. Biol*. 49:111–119, 2004.
[191]Terasaki, H., Y. Miyake, and S. Awaya. Fluorescein angiography of peripheral retina and pars plana during vitrectomy for proliferative diabetic retinopathy. *Am. J. Ophthalmol*. 123:370–376, 1997.
[192]Theer, P., M. T. Hasan, and W. Denk. Two-photon imaging to a depth of 1000 mu m in living brains by use of

a Ti : Al2O3 regenerative amplifier. *Opt. Lett.* 28:1022–1024, 2003.
[193]Thekkek, N., and R. Richards-Kortum. Optical imaging for cervical cancer detection: solutions for a continuing global problem. *Nat. Rev. Cancer* 8:725–731, 2008.
[194]Themelis, G., J. S. Yoo, K. Soh, R. B. Schulz, and V. Ntziachristos. Real-time intraoperative fluorescence imaging system using light-absorption correction (Journal Paper). *J. Biomed. Opt.* 14:064012, 2009.
[195]Thiberville, L., M. Salaun, S. Lachkar, S. Dominique, S. Moreno-Swirc, C. Vever-Bizet, and G. Bourg-Heckly. Confocal fluorescence endomicroscopy of the human airways. *Proc. Am. Thorac. Soc.* 6:444–449, 2009.
[196]Thong, P. S., M. Olivo, K. W. Kho, W. Zheng, K. Mancer, M. Harris, and K. C. Soo. Laser confocal endomicroscopy as a novel technique for fluorescence diagnostic imaging of the oral cavity. *J. Biomed. Opt.* 12:014007, 2007.
[197]Thorling, C. A., Y. Dancik, C. W. Hupple, G. Medley, X. Liu, A. V. Zvyagin, T. A. Robertson, F. J. Burczynski, and M. S. Roberts. Multiphoton microscopy and fluorescence lifetime imaging provide a novel method in studying drug distribution and metabolism in the rat liver in vivo. *J. Biomed. Opt.* 16:086013, 2011.
[198]Tong, L., Q. Wei, A. Wei, and J.-X. Cheng. Gold nanorods as contrast agents for biological imaging: optical properties, surface conjugation and photothermal effects. *Photochem. Photobiol.* 85:21–32, 2009.
[199]Tonn, J. C., and W. Stummer. Fluorescence-guided resection of malignant gliomas using 5-aminolevulinic acid: practical use, risks, and pitfalls. *Clin. Neurosurg.* 55:20–26, 2008.
[200]Tosi, A., A. Dalla Mora, F. Zappa, A. Gulinatti, D. Contini, A. Pifferi, L. Spinelli, A. Torricelli, and R. Cubeddu. Fast-gated single-photon counting technique widens dynamic range and speeds up acquisition time in time-resolved measurements. *Opt. Express* 19:10735–10746, 2011.
[201]Trattnig, S., K. Pinker, A. Ba-Ssalamah, and I. M. Nobauer-Huhmann. The optimal use of contrast agents at high field MRI. *Eur. Radiol.* 16:1280–1287, 2006.
[202]Troyan, S. L., V. Kianzad, S. L. Gibbs-Strauss, S. Gioux, A. Matsui, R. Oketokoun, L. Ngo, A. Khamene, F. Azar, and J. V. Frangioni. The FLARE intraoperative near-infrared fluorescence imaging system: a first-in-human clinical trial in breast cancer sentinel lymph node mapping. *Ann. Surg. Oncol.* 16:2943–2952, 2009.
[203]Uchiyama, K., M. Ueno, S. Ozawa, S. Kiriyama, Y. Shigekawa, and H. Yamaue. Combined use of contrast-enhanced intraoperative ultrasonography and a fluorescence navigation system for identifying hepatic metastases. *World J. Surg.* 34:2953–2959, 2010.
[204]Van Dam, G. M., G. Themelis, L. M. Crane, N. Harlaar, J. S. De Jong, H. J. Arts, J. Bart, P. Low, and V. Ntziachristos. Intraoperative tumor-specific fluorescence imaging in ovarian cancer by folate receptor-α targeting: first in-human results. *Nat. Med.* 17:1315–1349, 2011.
[205]Vargas, G., T. Shilagard, K. H. Ho, and S. McCammon. Multiphoton autofluorescence microscopy and second harmonic generation microscopy of oral epithelial neoplasms. Annual International Conference of the IEEE Engineering in Medicine and Biology Society, pp. 6311–6313, 2009.
[206]Venkatesh, K., M. Cohen, C. Evans, P. Delaney, S. Thomas, C. Taylor, A. Abou-Taleb, R. Kiesslich, and M. Thomson. Feasibility of confocal endomicroscopy in the diagnosis of pediatric gastrointestinal disorders. *World J. Gastroenterol.* 15:2214–2219, 2009.
[207]Vinegoni, C., T. Ralston, W. Tan, W. Luo, D. L. Marks, and S. A. Boppart. Integrated structural and functional optical imaging combining spectral-domain optical coherence and multiphoton microscopy. *Appl. Phys. Lett.* 88:053901, 2006.
[208]Wada, Y., S. E. Kudo, H. Kashida, N. Ikehara, H. Inoue, F. Yamamura, K. Ohtsuka, and S. Hamatani. Diagnosis of colorectal lesions with the magnifying narrow-band imaging system. *Gastrointest. Endosc.* 70:522–531, 2009.
[209]Wang, H. W., Y. Fu, T. B. Huff, T. T. Le, H. Wang, and J. X. Cheng. Chasing lipids in health and diseases by coherent anti-Stokes Raman scattering microscopy. *Vib. Spectrosc.* 50:160–167, 2009.
[210]Waseda, K., J. Ako, T. Hasegawa, Y. Shimada, F. Ikeno, T. Ishikawa, Y. Demura, K. Hatada, P. G. Yock, Y. Honda, P. J. Fitzgerald, and M. Takahashi. Intraoperative fluorescence imaging system for on-site assessment of off-pump coronary artery bypass graft. *JACC Cardiovasc. Imaging* 2:604–612, 2009.
[211]Widhalm, G., S. Wolfsberger, G. Minchev, A. Woehrer, M. Krssak, T. Czech, D. Prayer, S. Asenbaum, J. A. Hainfellner, and E. Knosp. 5 Aminolevulinic acid is a promising marker for detection of anaplastic foci in diffusely infiltrating gliomas with nonsignificant contrast enhancement. *Cancer* 116:1545–1552, 2010.
[212]Witjes, J. A., and J. Douglass. The role of hexaminolevulinate fluorescence cystoscopy in bladder cancer. Nature clinical practice. *Urology* 4:542–549, 2007.
[213]Witjes, J. A., J. P. Redorta, D. Jacqmin, F. Sofras, P. U. Malmstrom, C. Riedl, D. Jocham, G. Conti, F. Montorsi, H. C. Arentsen, D. Zaak, A. H. Mostafid, and M. Babjuk. Hexaminolevulinate-guided fluorescence cystoscopy in the diagnosis and follow-up of patients with non-muscle-invasive bladder cancer: review of the evidence and recommendations. *Eur. Urol.* 57:607–614, 2010.
[214]Wolfsen, H. C., J. E. Crook, M. Krishna, S. R. Achem, K. R. Devault, E. P. Bouras, D. S. Loeb, M. E. Stark, T. A. Woodward, L. L. Hemminger, F. K. Cayer, and M. B. Wallace. Prospective, controlled tandem endoscopy study of narrow band imaging for dysplasia detection in Barrett's Esophagus. *Gastroenterology* 135:24–31, 2008.
[215]Won, Y., S. Hong, H. Yu, Y. Kwon, S. Yun, S. Lee, and J. Lee. Photodetection of basal cell carcinoma using methyl 5 aminolaevulinate induced protoporphyrin IX based on fluorescence image analysis. *Clin. Exp. Dermatol.* 32:423–429, 2007.
[216]Xu, C., J. M. Schmitt, T. Akasaka, T. Kubo, and K. Huang. Automatic detection of stent struts with thick neointimal growth in intravascular optical coherence tomography image sequences. *Phys. Med. Biol.* 56:6665–6675, 2011.
[217]Yang, J. M., K. Maslov, H. C. Yang, Q. Zhou, K. K. Shung, and L. V. Wang. Photoacoustic endoscopy. *Opt. Lett.* 34:1591–1593, 2009.
[218]Yang, V. X., S. J. Tang, M. L. Gordon, B. Qi, G. Gardiner, M. Cirocco, P. Kortan, G. B. Haber, G. Kandel, I. A. Vitkin, B. C. Wilson, and N. E. Marcon. Endoscopic Doppler optical coherence tomography in the human GI tract: initial experience. *Gastrointest. Endosc.* 61:879–890, 2005.
[219]Yi, K., M. Mujat, B. H. Park, W. Sun, J. W. Miller, J. M. Seddon, L. H. Young, J. F. de Boer, and T. C. Chen.

Spectral domain optical coherence tomography for quantitative evaluation of drusen and associated structural changes in non-neovascular age-related macular degeneration. *Br. J. Ophthalmol*. 93:176–181, 2009.

[220]Zargi, M., I. Fajdiga, and L. Smid. Autofluorescence imaging in the diagnosis of laryngeal cancer. *Eur. Arch. Otorhinolaryngol*. 257:17–23, 2000.

[221]Zaric, B., H. D. Becker, B. Perin, A. Jovelic, G. Stojanovic, M. D. Ilic, Z. Eri, M. Panjkovic, D. Obradovic, and M. Antonic. Narrow band imaging videobronchoscopy improves assessment of lung cancer extension and influences therapeutic strategy. *Jpn. J. Clin. Oncol*. 39:657–663, 2009.

[222]Zhao, B. Z., and Y. Y. He. Recent advances in the prevention and treatment of skin cancer using photodynamic therapy. *Expert Rev. Anticancer Ther*. 10:1797–1809, 2010.

[223]Zhao, Y., H. Nakamura, and R. J. Gordon. Development of a versatile two-photon endoscope for biological imaging. *Biomed. Opt. Express* 1:1159–1172, 2010.

[224]Zheng, W., M. Harris, K. W. Kho, P. S. Thong, A. Hibbs, M. Olivo, and K. C. Soo. Confocal endomicroscopic imaging of normal and neoplastic human tongue tissue using ALA-induced-PPIX fluorescence: a preliminary study. *Oncol. Rep*. 12:397–401, 2004.

[225]Zhu, J., B. Lee, K. K. Buhman, and J. X. Cheng. A dynamic, cytoplasmic triacylglycerol pool in enterocytes revealed by ex vivo and in vivo coherent anti-Stokes Raman scattering imaging. *J. Lipid Res*. 50:1080–1089, 2009.

[226]Zimmerley, M., C. Y. Lin, D. C. Oertel, J. M. Marsh, J. L. Ward, and E. O. Potma. Quantitative detection of chemical compounds in human hair with coherent anti-Stokes Raman scattering microscopy. *J. Biomed. Opt*. 14:044019, 2009.

[227]Zysk, A. M., F. T. Nguyen, A. L. Oldenburg, D. L. Marks, and S. A. Boppart. Optical coherence tomography: a review of clinical development from bench to bedside. *J. Biomed. Opt*. 12:051403, 2007.